

AD-766 771

MEASUREMENT OF STRESS STATES IN 20 X 4.4  
AIRCRAFT TIRE

Samuel K. Clark, et al

Michigan University

Prepared for:

Air Force Flight Dynamics Laboratory

February 1973

DISTRIBUTED BY:

**NTIS**

National Technical Information Service  
U. S. DEPARTMENT OF COMMERCE  
5285 Port Royal Road, Springfield Va. 22151

AFFDL-TR-73-24

1

ame

# MEASUREMENT OF STRESS STATES IN 20 x 4.4 AIRCRAFT TIRE

SAMUEL K. CLARK  
RICHARD N. DODGE  
DONALD LEE  
RICHARD LARSON

*The University of Michigan*



TECHNICAL REPORT AFFDL-TR-73-24

FEBRUARY 1973

Reproduced by  
NATIONAL TECHNICAL  
INFORMATION SERVICE  
U S Department of Commerce  
Springfield VA 22151

Approved for public release; distribution unlimited

AIR FORCE FLIGHT DYNAMICS LABORATORY  
AIR FORCE SYSTEMS COMMAND  
WRIGHT-PATTERSON AIR FORCE BASE, OHIO

AD 766771

# NOTICES

When Government drawings, specifications, or other data are used for any purpose other than in connection with a definitely related Government procurement operation, the United States Government thereby incurs no responsibility nor any obligation whatsoever; and the fact that the Government may have formulated, furnished, or in any way supplied the said drawings, specifications, or other data, is not to be regarded by implication or otherwise as in any manner licensing the holder or any other person or corporation, or conveying any rights or permission to manufacture, use, or sell any patented invention that may in any way be related thereto.

ACCESSION for	
NTIS	White Section <input checked="" type="checkbox"/>
DDC	Buff Section <input type="checkbox"/>
UNANNOUNCED	<input type="checkbox"/>
JUSTIFICATION	
BY	
DISTRIBUTION/AVAILABILITY CODES	
Dist.	AVAIL. BY
A	

Copies of this report should not be returned unless return is required by security considerations, contractual obligations, or notice on a specific document.

**AFFDL-TR-73-24**

**MEASUREMENT OF STRESS STATES IN  
20 x 4.4 AIRCRAFT TIRE**

*SAMUEL K. CLARK  
RICHARD N. DODGE  
DONALD LEE  
RICHARD LARSON*

Approved for public release; distribution unlimited

## FOREWORD

This work was performed by the Department of Engineering Mechanics, College of Engineering, The University of Michigan, Ann Arbor, Michigan under United States Air Force Contract No. F33615-72-C-1004. The contract was initiated under Project 1369, "Mechanical Subsystems for Advanced Military Flight Vehicles" and Task No. 136903, "Landing Gear System Ground Contact Components for Advanced Military Flight Vehicles." The work was conducted under the direction of the Vehicle Equipment Division, Air Force Flight Dynamics Laboratory, Wright-Patterson Air Force Base, Ohio, Dr. H. K. Brewer (FEM), Project Engineer. This report covers work performed from August 1971 to December 1972.

The authors would like to acknowledge the cooperation of the B. F. Goodrich Tire Company in contracting to build one 20 x 4.4 aircraft tire for test purposes. We would also like to give special thanks to Air Treads, Inc. of Atlanta, Georgia, and to Mr. W. C. Shaver and Mr. Henry Brown of Air Treads for their kindness and cooperation in allowing us to retread a number of aircraft tires in their facilities.

Publication of this technical report does not constitute Air Force approval of the report's findings or conclusions. It is published only for the exchange and stimulation of ideas.

This technical report has been reviewed and is approved.



Kennerly H. Digges  
Chief, Mechanical Branch  
Vehicle Equipment Division  
Air Force Flight Dynamics Laboratory

# ABSTRACT

Measurements were made on the stress state at the tread-carcass interface on a 20 x 4.4 Type VII 12 PR aircraft tire operating on curved surfaces simulating a number of different roadwheel diameters. The general results of these measurements show that the stress levels in the tire increase as the roadwheel diameters decrease, using the adjusted pressure schedules given in Figure 5 of MIL-T-5041F, and that in all cases the stress levels are higher on curved roadwheels than on a flat surface such as a runway.

## TABLE OF CONTENTS

	Page
SUMMARY	vii
NORMAL STRESS MEASUREMENTS	1
SHEAR STRESS MEASUREMENTS	10
CORD LOAD MEASUREMENTS	16
TEMPERATURE MEASUREMENTS	28
SUMMARY OF STRESS STATE MEASUREMENTS	31
CONCLUSIONS AND RECOMMENDATIONS	32
REFERENCES	33
APPENDIX I: NORMAL STRESS TRANSDUCERS	34
APPENDIX II: SHEAR STRESS TRANSDUCERS	37
APPENDIX III: CORD LOAD TRANSDUCERS	40
APPENDIX IV: SIMULATED FLYWHEEL	42

## LIST OF ILLUSTRATIONS

Figure	Page
1. 20 x 4.4 Type VII Aircraft Tire Cross Section.	1
2. Normal Stress at Base of Rib 1 During Contact.	3
3. Normal Stress at Base of Rib 2 During Contact.	4
4. Peak Normal Stress Levels at Various Roadwheel Diameters.	8
5. Average Normal Stress in the Contact Region at Various Roadwheel Diameters.	9
6A. Axial Shear Stress at Tread Base as Tire Rolls Through Contact.	11
6B. Circumferential Shear Stress at Tread Base During Rolling Through the Contact Patch.	11
7. Free Body Diagram of Section of Tread Rib.	13
8. Circumferential Shear Stress at Tread Base as Tire Rolls Through Contact.	14
9. Circumferential Normal Stress vs. Position as Tire Rolls Through the Contact Patch.	15
10. Cord Load vs. Inflation Pressure, Plies 1 and 2.	18
11. Cord Load vs. Inflation Pressure, Plies 3 and 4.	19
12. Cord Load vs. Inflation Pressure, Plies 5 and 6.	20
13. Cord Load vs. Inflation Pressure, Plies 7, 8, and 9.	21
14. Cord Load Transducer Locations	22
15. Calibration of Cord Load Transducers—Output Signal vs. Cord Load	23
16. Contact Patch Length, as Measured by Signal Bandwidth from Cord Load Transducers, for Various Roadwheel Diameters.	24
17. Peak Cord Load for Various Roadwheel Diameters.	25
18. Minimum Cord Load for Various Roadwheel Diameters.	26



# LIST OF ILLUSTRATIONS (Concluded)

Figure		Page
19.	Alternating Cord Load for Various Roadwheel Diameters.	27
20.	Tire Temperature Buildup During Taxi-Takeoff Cycle.	29
21.	Tire Temperature Buildup During Two-Mile Break-In Run.	30
22.	Sensing Face of Normal Stress Transducer.	34
23.	Edge View of Normal Stress Transducer.	35
24.	Calibration Fixture for Normal Stress Transducer, Disassembled.	36
25.	Shear Stress Transducer Geometry.	37
26.	Photograph of Shear Stress Transducer.	38
27.	Shear Stress Calibration Fixture.	38
28.	Rubber Beam Used to Calibrate Shear Stress Transducers.	39
29.	Free Body Diagram of Section of Tire Carcass.	40
30.	Tubular Cord Load Transducer.	41
31.	Schematic Drawing of Device to Simulate a Roadwheel.	42
32.	Photograph of Test Tire Loaded Against a Simulated Roadwheel.	44

Table		Page
I.	INFLATION PRESSURES FOR VARIOUS ROADWHEEL DIAMETERS	5
II.	PEAK NORMAL STRESS VALUES (NORMALIZED)	6
III.	PEAK NORMAL STRESS VALUES (NORMALIZED)	6
IV.	AXIAL SHEAR STRESS	10
V.	CIRCUMFERENTIAL SHEAR STRESS	12
VI.	CIRCUMFERENTIAL SHEAR STRESS	13

## SUMMARY

The knowledge of the stress state in pneumatic tires is important because it determines such factors as tire cord fatigue life, the development of separations between various elements used in the tire, and the buildup of heat in the tire. Increased temperature degrades both the ultimate strength and fatigue life characteristics of all tire materials. In addition, there is little question but that flaws or areas of incipient weakness in the tire may not result in premature tire failure if such areas are located in regions of relatively low fluctuating stress, while the very same weaknesses or incipient flaws may cause premature tire failure or over-heating, provided that they are located in regions of relatively high stress. Hence the stress state is important in a general sense in tire technology, even though modern cord strengths are sufficient so that the so-called "blow out" or complete cord rupture is no longer a common occurrence in service. Finally, a knowledge of such stress states is important in qualification testing of tires since all qualification testing is carried out on dynamometer wheels whose curvature is different from that of the runway on which the tire normally operates in service. Hence, adjustment of tire load and pressure on dynamometer wheels should ideally be carried out on the basis of maximum induced tire stress, since this is the criterion most closely allied to tread separation or other tire failures.

So far the knowledge of internal stresses in tires is relatively limited. What information exists comes from two sources. The first of these is direct calculation of various mathematical models, chosen to represent the pneumatic tire as closely as possible. For the most part these models are far too crude to indicate the nature of the detailed stress state in the tire, or even the average stress state in any condition other than that of direct tire inflation. Almost no good mathematical models are available for the influence of road-wheel or dynamometer curvature, or for the influence of tire speed and deflection. For this reason the present state of stress analysis of tires from an analytical point of view is very rudimentary and of little use in adjusting loads and inflation pressures for qualification testing.

A somewhat more fruitful avenue of examination of tire stress states has been carried out through the mechanism of various experiments using different kinds of sensors or strain measuring devices on tires directly. Several different approaches have been used here. In some of the earlier work various kinds of strain measuring sensors were attached to both the inside and outside surface of the tire in an attempt to measure tire surface strains, and from these to deduce the nature of the internal stress state. Outstanding work in this area has been done by Kern [1] and by Janssen and Walter [2]. Kern used metallic gages based upon the resistance strain gage principle, in the form often called a "clip gage" in this country. Janssen and Walter used small rubber tubing with a capillary hole filled with a liquid metal, bonded to the inside of the tire.

Both of these methods just described for measuring the strain on the surface of the tire require that one interpret these strains backward into internal stress state in the tire. This is not particularly easy in the case of a composite structure with greatly different moduli of elasticity, as is the case with a pneumatic tire. It is not at all clear that the internal strain state can be related to the surface strain state in a fashion as simple as in isotropic materials, where the Kirchhoff hypothesis is known to be fairly exact. There is, in fact, some evidence that the Kirchhoff hypothesis does not apply in the case of textile cords embedded in rubber, and so considerable uncertainty is associated with the process of interpreting strain measurements in terms of internal stress states.

A more direct approach has been to measure tire cord loads by instrumentation attached directly to the tire cords inside the tire. This approach has been used by Walter [3], by Clark and Dodge [4], and by Dodge, Larson, and Clark [5]. In some respects this method has advantages since miniature transducers are now available which can measure the cord load at internal locations in the tire. However, no simple direct method has yet been developed to interpret cord load information in terms of interply shear stresses measured in the tire, or in terms of tendency for separations to occur in the tire, as for example in the case of tread separation. It would seem that on this basis cord load information alone would be of limited practical significance.

With this background, the Air Force Flight Dynamics Laboratory contracted with the Department of Engineering Mechanics at The University of Michigan in August 1971 to conduct an experimental stress analysis of a 20 x 4.4 Type VII aircraft tire with varying radius of curvatures of the dynamometer roadwheels upon which the tire was qualified. The express aim was to attempt to measure the stress state in this tire at the base of the tread of the tire. That particular area was chosen for detailed examination since this size of tire had experienced considerable difficulty with tread separation and chunking during qualification tests. Subsequent work carried out on this contract has been directed toward the measurement of the stress states throughout the tire carcass with the particular emphasis on the base of the tread, as indicated. Considering the interface between the tread and the uppermost fabric layer in the tire as a two-dimensional surface, the objective of this work was to determine both the normal stress and the shear stresses on this surface underneath the tread ribs of this tire.

## NORMAL STRESS MEASUREMENTS

It was decided to measure the stress component normal, or perpendicular, to the surface separating the uppermost fabric layer from the base of the tread by means of miniature strain gage pressure transducers embedded at various points in the tread close to the surface. Attention was concentrated on two main areas, the center rib just to one side of the central groove, as shown in Figure 1 and designated as "rib 1" and in the second major rib designated as "rib 2" in Figure 1.

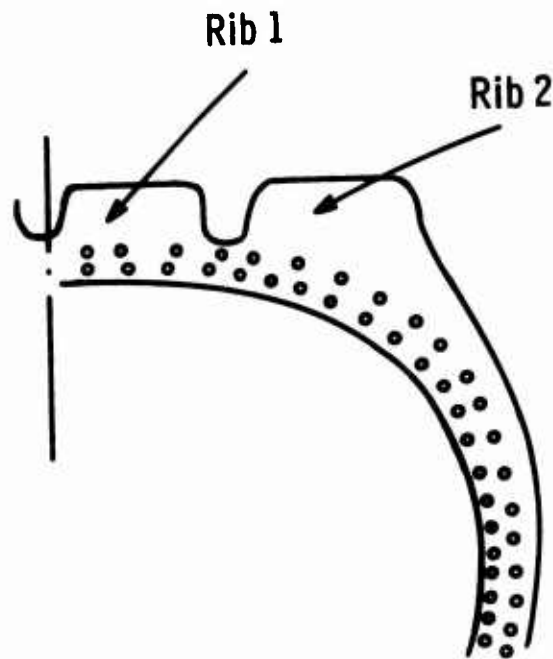


Figure 1. 20 x 4.4 Type VII Aircraft Tire Cross Section.

In order to make effective measurements of this type, the pressure transducers used should be relatively small in order to minimize the disruption of the local stress state in this area. A particularly small and yet relatively inexpensive form of transducer was devised for this purpose. Since its development and calibration occupied a substantial portion of the time and effort of this contract, no attempt will be made here to fully describe its geometry and mode of operation. This will be covered in Appendix I. In addition, the general relationship between signal output and absolute stress level will also be covered there since this represents another area of essentially separate development and calibration.

The miniature pressure transducers finally adopted for this work were approximately 0.125 in. in diameter and 0.030 in. thick. A number of them were

embedded at the base of the tread in different tires, all of the 20 x 4.4 size and all from a common manufacturer, the B. F. Goodrich Tire Company. Two methods for inserting or embedding the transducer were employed. In the first method, used only sparingly and primarily for calibration and trial purposes, a slit was cut from the side of the tire parallel to the tread surface but located in depth close to the tread base. The transducer was then pushed into this slit and the entire slit sealed back up with some suitable bonding agent. While the system did give results generally compatible with other methods of embedding transducers, it nevertheless was not considered to be completely satisfactory.

A system for inserting transducers much better suited to the objectives of this work was based upon buffing these tires in a retreading shop as close to the surface of the upper layer of tire fabric as possible. Prior to recapping, the pressure transducers were bonded to the buffed surface of the tire and their lead wires brought out through the side. The recapping tread was then stripped on using an Orbitread process and the resulting tire cured in a mold in the normal fashion. The pressure transducer was designed to withstand the temperatures and pressures used during the cure process, so that after the cured tire was removed from the mold, the pressure transducers were available for the measurement of internal stresses in the tire.

One major difficulty associated with the process of curing pressure transducers into a tire lies in the difficulty in determining completely their exact location and orientation after the cure process has been completed. This represents a relatively severe problem for the experimentalist since the stresses obtained from them are extremely sensitive to their angular orientation, and somewhat less sensitive to their lateral position across the cross section of the tire. For this reason it was not possible to definitely ascertain the exact position of the pressure sensors underneath each of the ribs as shown in Figure 1. Thus, the data obtained is only listed as occurring in rib 1 or in rib 2, due allowance given to small motion of the transducer during the cure process in retreading.

Due to small angular differences in position, some scatter appears in the data. However, the general trends of the data are uniform enough so that this does little more than change the general level of magnitude of the pressures observed.

To some extent the normal stress measurements parallel the pressure distribution in the footprint of the tire. Wide differences are observed between the normal stresses taken on rib 1 and on rib 2, over the various conditions utilized here. For example, Figure 2 shows a typical normal stress measurement taken on rib 1 as the tire rolls through the contact patch. This is similar in many respects to the type of contact pressure distribution curves observed near the center of an aircraft tire, as has been shown in [6]. Figure 3 is a normal

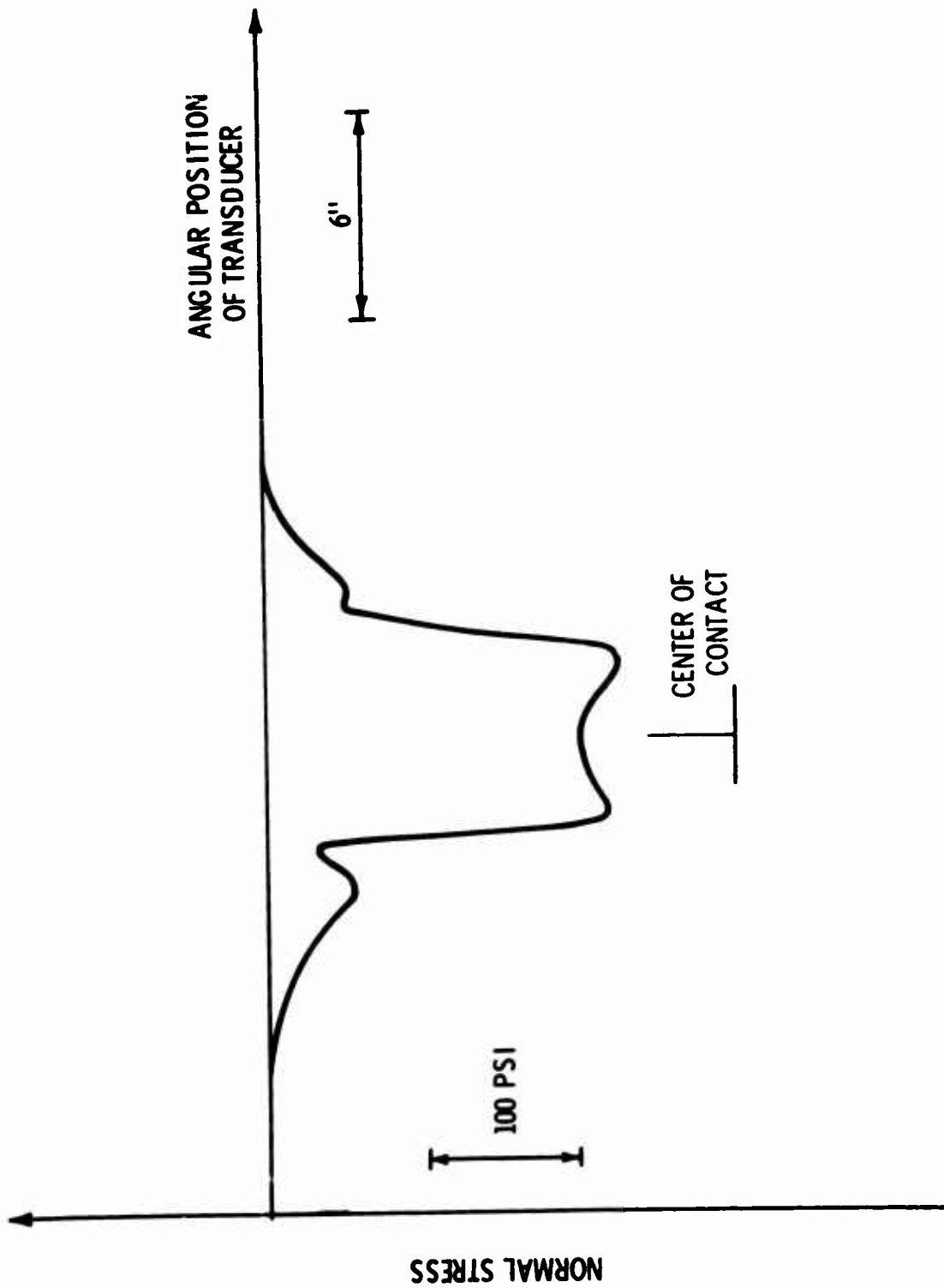


Figure 2. Normal Stress at Base of Rib 1 During Contact.

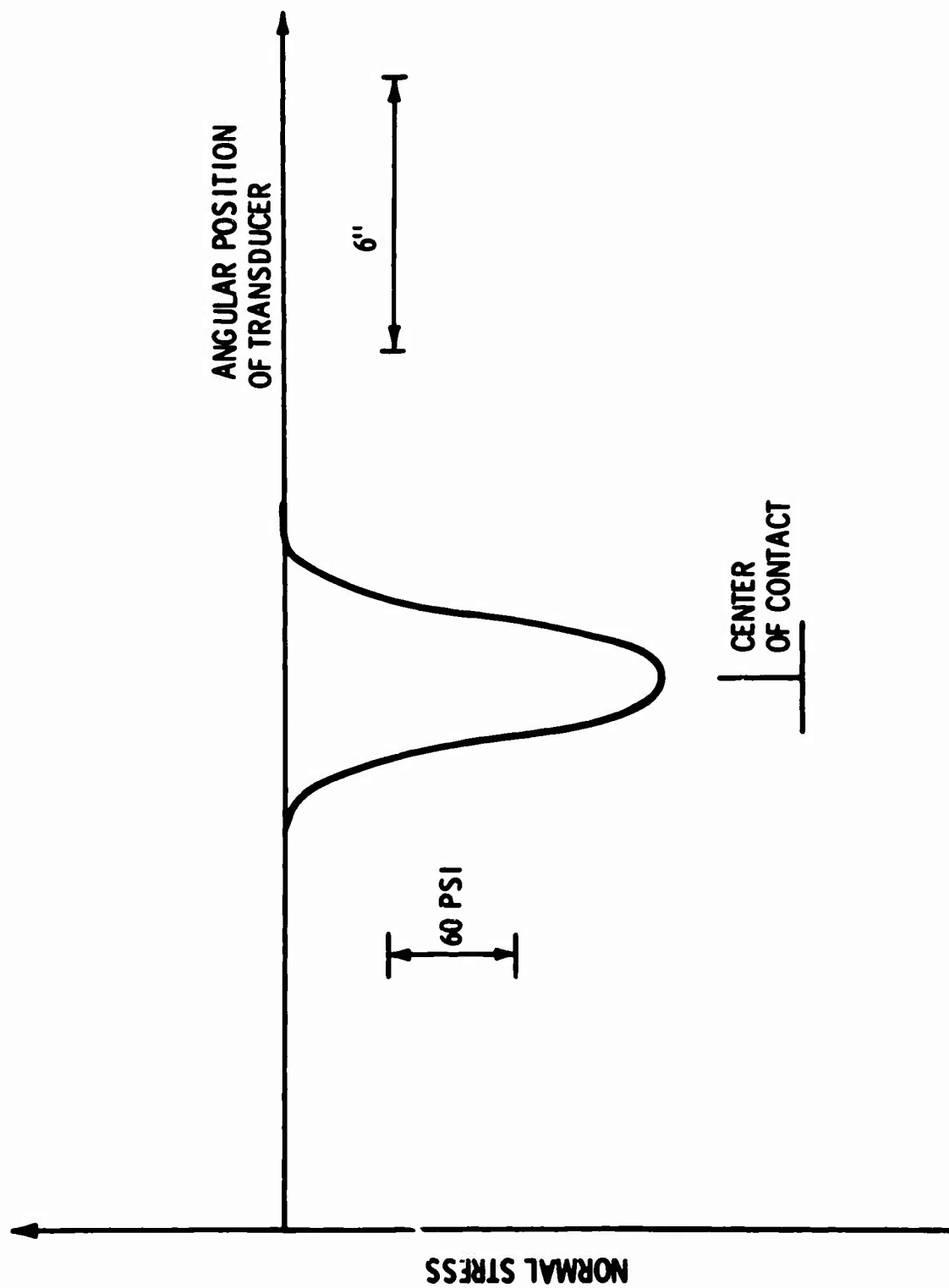


Figure 3. Normal Stress at Base of Rib 2 During Contact.

stress curve taken as the tire rolls through contact, measured at the base of the tread on rib 2. This type of behavior has also been previously observed in contact pressure curves.

The principle objective of this study was to compare the stress states under varying conditions of radii of curvature and inflation pressure prescribed by MIL-T-5041F, Figure 5, where the chart for adjusting aircraft tire test inflation pressures for flywheel curvature gives a technique for increasing inflation pressure to compensate for varying flywheel curvatures.

The rated load for this tire is 5150 lb at a rated flat plate inflation pressure of 225 psi. Due to lack of proper equipment for obtaining 225 psi inflation safely, it was agreed to reduce the flat plate inflation pressure for these tests to 150 psi with a corresponding load change to achieve the same tire deflection as under rated conditions, namely, 1.0 in. Variations of roadwheel diameter were then obtained by varying inflation pressure according to Figure 5 of MIL-T-5041F. In the particular case at hand, five separate flywheel curvatures were simulated. These were 67.30-in. diameter, 84-in. diameter, 120-in. diameter, 192-in. diameter, and the flat plate. The tire inflation pressures chosen for these tests are indicated in Table I.

TABLE I  
INFLATION PRESSURES FOR VARIOUS ROADWHEEL DIAMETERS

Flywheel Diameter, in.	Inflation Pressure, psi	Load, lb
Flat Plate	150	3100
192	150	3100
120	160	3100
84	166.5	3100
67.3	170	3100

Using the modified inflation pressures as recommended by MIL-T-5041F, the general results of the normal stress measurements indicate clearly that the peak normal stress level at the base of the tread increases as the diameter of the flywheel decreases. They may be seen from Table II, where a series of measurements is reported on a normalized basis, that is to say, where the flat plate peak stress level is adjusted to a value of 100. From this it may be seen that over a large number of measurements the resulting increase in peak stress seems to be reasonably uniform, allowing for some variation in the measurement process.



TABLE II

## PEAK NORMAL STRESS VALUES (NORMALIZED)

Rib	Sensor	Flywheel Diameter, in.				
		Flat Plate	192	120	84	67.3
1	A-27	100	100	102	108	111
1	C-19	100	103	108	113	116
1	A-34	100	105	110	117	125
1	C-18	100	108	113	118	120
1	A-23	100	102	109	111	118
2	C-16	100	101	106	111	110
2	A-25	100	109	109	135	122
2	A-26	100	107	126	130	137
2	A-22	100	110	113	113	90

Similar data is given for a second tire in Table III, where again the data is presented in a normalized fashion as in Table II.

TABLE III

## PEAK NORMAL STRESS VALUES (NORMALIZED)

Rib	Sensor	Flywheel Diameter, in.				
		Flat Plate	192	120	84	67.3
1	A-21	100	101	103	107	109
1	A-30	100	101	107	109	114
1	C-8	100	98.5	106	111	117
1	A-20	100	104	107.5	111	114
2	C-15	100	101	109	118	123
2	A-33	100	113	121	118	124
2	C-6	100	96	101	103	103

From a study of these two tables it is quite clear that the present inflation schedule for decreasing flywheel diameter penalizes those tests run on flywheels, particularly smaller ones. There are many instances in Tables II and II of normal stresses on smaller diameter flywheels being 20 percent above those encountered under similar conditions of flat plate loading. As might be expected, this could result in premature fatigue

failure of a tire which would not otherwise fail in service. The slopes of fatigue curves may be extremely shallow, and it is entirely possible that even 20 percent difference in the normal stress state at the base of the tread would be sufficient to cause the alternating stress component associated with this value to increase to the point where premature failure occurred.

In computing the peak stress levels shown in Tables II and III, it was assumed that the stress level at the base of the tread outside of the contact patch was essentially zero. Under high-speed running conditions it might very well have some positive tensile value, as opposed to the compressive levels measured with the pressure sensors and reported in Tables II and III.

The absolute values of the peak normal stress levels measured in these experiments using the miniature pressure transducers are of less interest, but are included for completeness. This information is presented in Figure 4 as the normal stress component perpendicular to the tire carcass at the tread base, as a function of flywheel diameter and for various sensors used in these experiments. These show stress levels generally ranging from approximately 100 to approximately 300 psi depending upon location and the particular sensor. In general the stress levels on the center ribs seem to be relatively consistent and regular. The reasons for the rather wide disparity between the two measurements taken on the outside ribs, at the extreme low and extreme high values of the data, are not known. It is probable that tipping and displacement of the pressure transducers during recapping may have been partly responsible for this rather wide difference in absolute stress level.

It is also important to note that the average stress level over the contact patch increases as the roadwheel diameter decreases. This is shown in Figure 5 where the average normal stress is plotted for different roadwheel diameters. This value is important since it reflects on two tire characteristics which bear strongly on durability and endurance life:

- (a) Tire temperature buildup.
- (b) Strain rate effects in the viscoelastic tire carcass and tread, where increased strain rates cause increased internal stress levels.

The length of the contact patch can be measured from these experimental records and clearly decreases as the roadwheel diameter decreases.

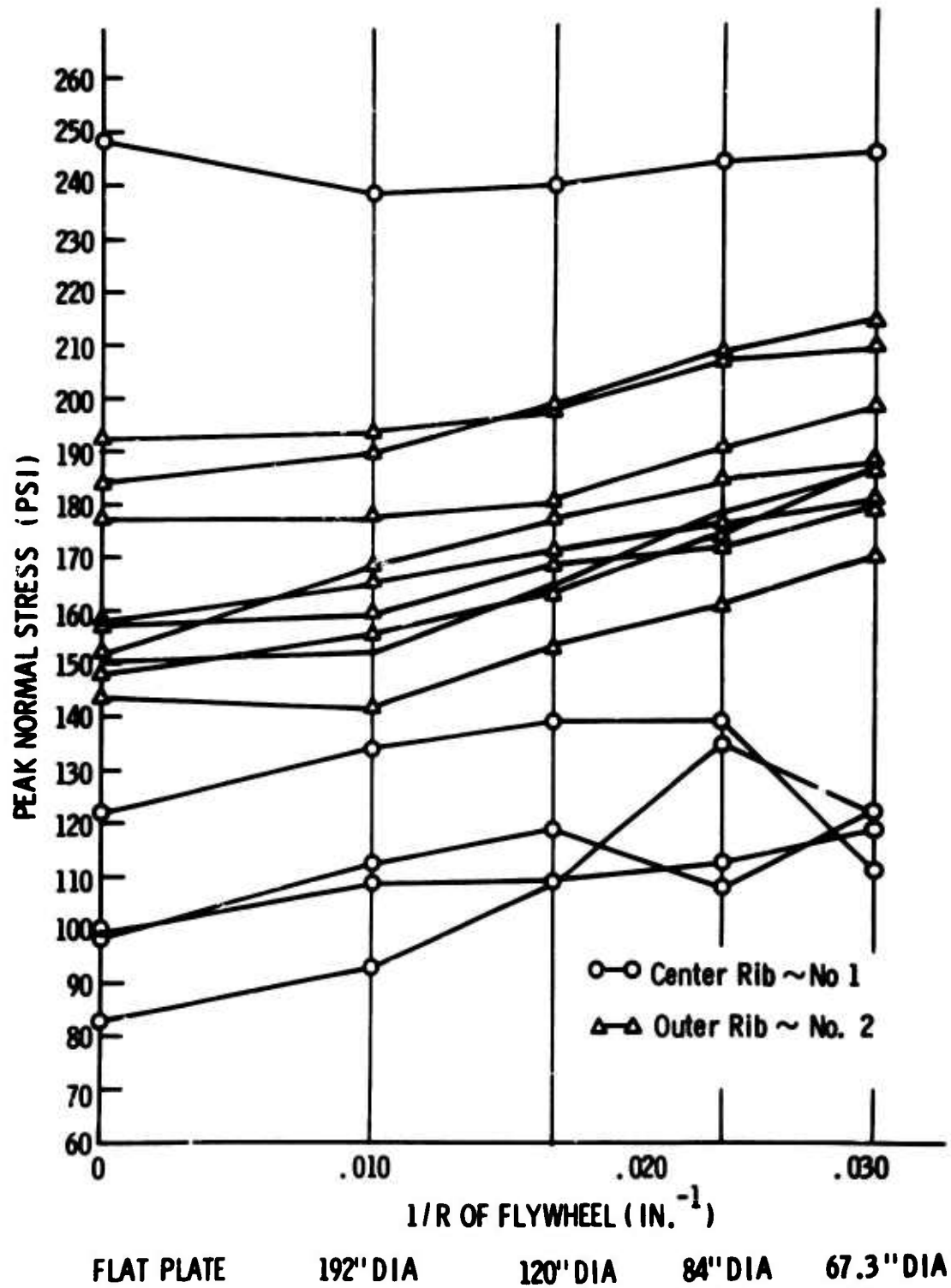


Figure 4. Peak Normal Stress Levels at Various Roadwheel Diameters.

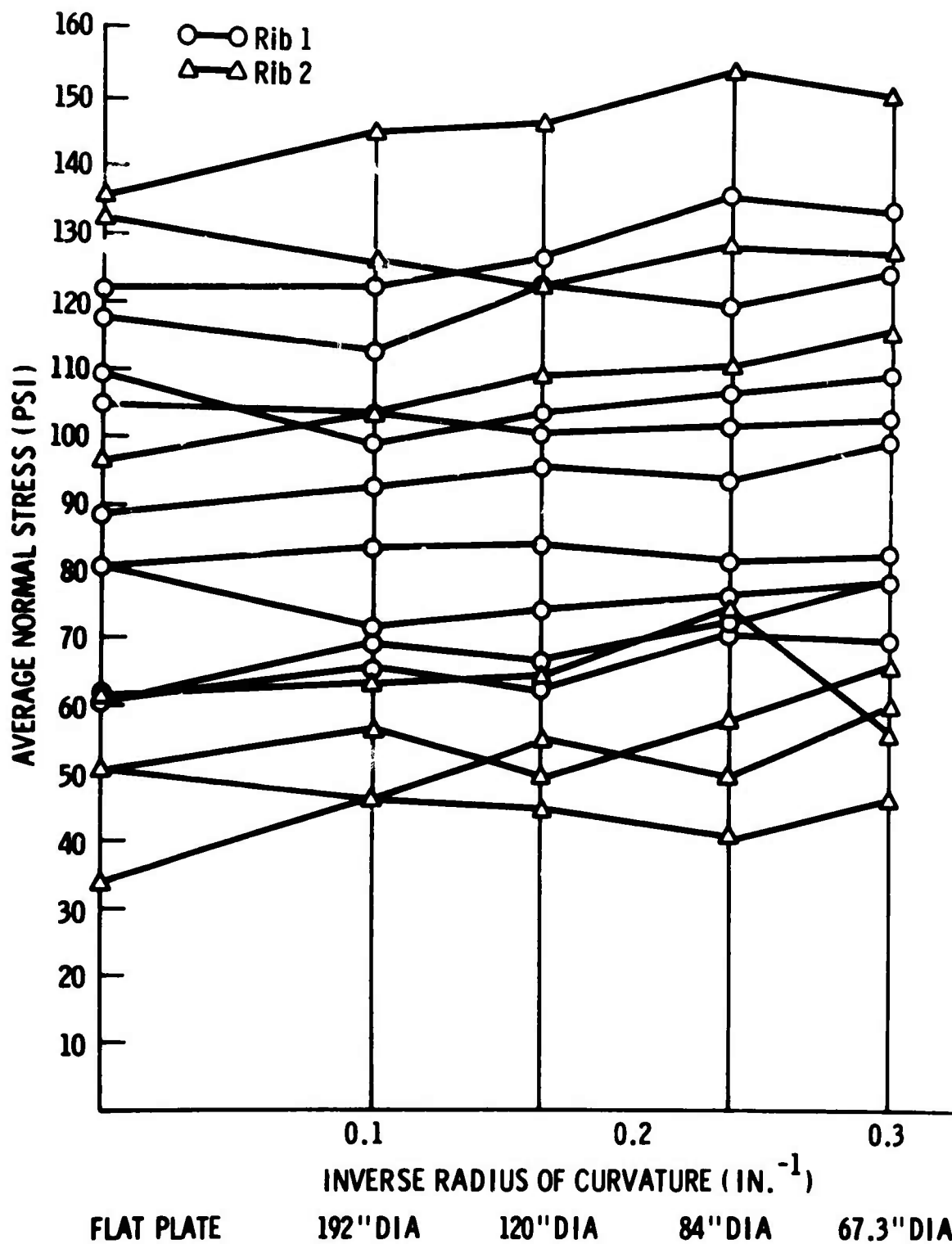


Figure 5. Average Normal Stress in the Contact Region at Various Roadwheel Diameters.

## SHEAR STRESS MEASUREMENTS

The tangential component of stress at the base of the tread can be separated into two components, one parallel to the axle of the wheel upon which the tire is mounted and one in the circumferential direction, parallel to the tread grooves. Two different techniques were used to measure the shear stress level at this location. The first of these, described more fully in a subsequent chapter of this report, used cord load transducers in an attempt to measure the carcass stress level through the entire tire. The application of equilibrium considerations will then give the value of the circumferential shear stress at the base of the tread. The second effort, described in this section of the report, used miniature shear strain transducers directly embedded in the base of the tread. These transducers were designed and made especially for this work, and so far as we know represent the first attempt to make such measurements. The transducers are more fully described, and their calibration processes are explained, in Appendix II of this report. For the moment the results gotten from them are presented here.

These shear strain transducers were designed in such a way that a small elastic beam in bending gave a signal proportional to the shear strain present at the location of the transducer, and in a particular direction with respect to the axis of the transducer. In the particular case to be described here, these axial shear strain transducers were placed in the base of rib 1 (see Figure 1) so that the shear strain in the axial direction at the base of that rib could be measured. Again using inflation pressures adjusted as indicated in Table I, the relative values of shear stress obtained from the base of rib 1 are given in Table IV.

TABLE IV

### AXIAL SHEAR STRESS

Rib	Flywheel Diameter, in.				
	Flat Plate	192	120	84	67.3
1	100	100	104	105	108

Here there is a tendency to increase the shear stress level as the diameter of the roadwheel decreases, just as in the normal stress data presented in the preceding section. A typical curve of axial shear stress vs. position along the contact patch is given in Figure 6A.

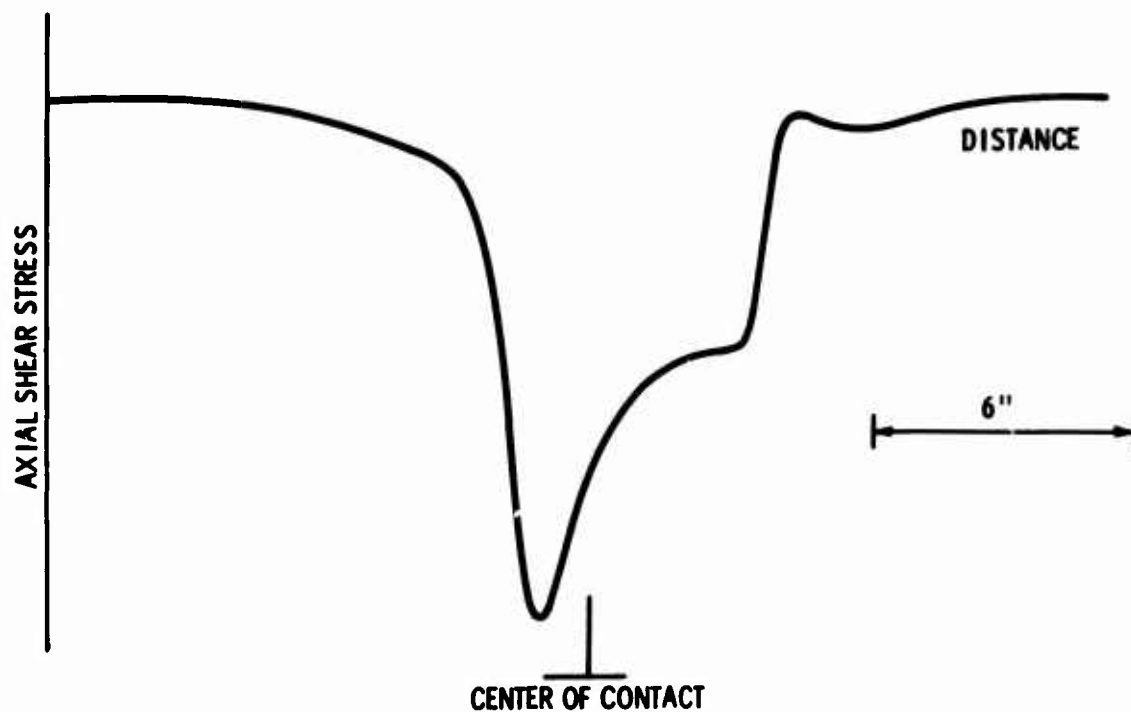


Figure 6A. Axial Stress at Tread Base as Tire Rolls Through Contact.



Figure 6B. Circumferential Shear Stress at Tread Base During Rolling Through the Contact Patch.

Next, data is presented on the shear stresses in the circumferential direction of the tire during rolling through the contact patch. These were obtained using the same kind of sensors but now with the sensor oriented in a direction parallel to the direction of tire tread grooves. Again rib 1 was chosen as the rib to be instrumented. The data obtained by this method is of questionable accuracy due to the lack of reproducibility of the transducer's signal, possibly caused by a bonding failure of the transducer to the tire carcass. The data is given in Table V.

TABLE V  
CIRCUMFERENTIAL SHEAR STRESS

Rib	Flywheel Diameter, in.				
	Flat Plate	192	120	84	67.3
1	100	111	105	101	104

A typical curve of circumferential shear stress vs. position along the contact patch is given in Figure 6B. Notice the asymmetric form of this, as might be expected from a consideration of the deformation pattern.

A third type of effort to measure shear stresses at the base of the tread uses the free body diagram of a section of a tread rib as shown in Figure 7. Here a small length of a typical tread rib is cut out, and shown on it are the tensile stresses on either side of the section, the surface traction due to frictional effects and the circumferential component of the tangential stress, or shear stress, at the tread base. This latter value is, of course, an average value as are the other stress components shown. For that reason the length of the segment should be considered rather small. Force equilibrium as shown below in Eq. (1) yields an expression for tangential shear stress  $\tau_{zx}$  as in Eq. (2).

$$b \cdot h \left( \sigma_x + \frac{\partial \sigma_x}{\partial x} \Delta x - \sigma_x \right) + T_{zx} b \Delta x - \tau_{zx} b \Delta x = 0 \quad (1)$$

In cases where the surface traction  $T_{zx}$  vanishes, one can solve for the tangential stress component in the form

$$\tau_{zx} = h \frac{\partial \sigma_x}{\partial x} \quad (2)$$

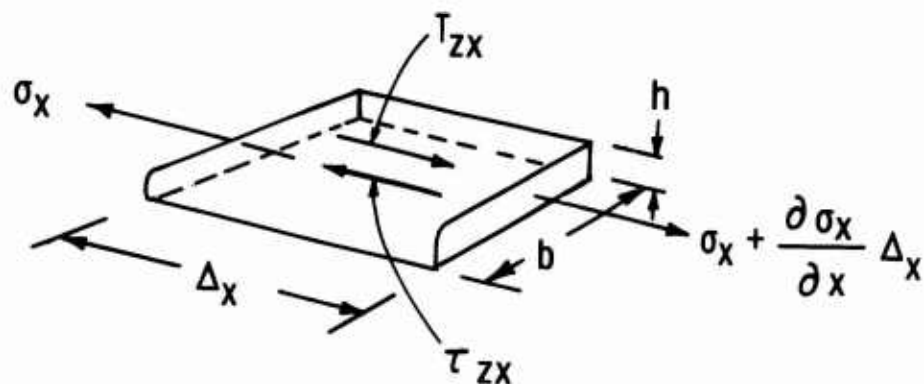


Figure 7. Free Body Diagram of Section of Tread Rib.

By suitable orientation of the miniature pressure transducers used to measure normal stress, one may measure the normal stress  $\sigma_x$  parallel to the tread surface. If this signal is recorded as the tire moves through the contact patch, one has a plot of  $\sigma_x$  vs.  $x$  for all positions of the tire at a fixed or stationary position of the tire. This signal or plot of  $\sigma_x$  can then be differentiated in order to obtain the required shear stress. This represents an independent method of obtaining the circumferential shear stress at the tread base.

These measurements were carried out using the miniature pressure transducer previously described, and the results are given in Figure 8 and Table VI, while a typical recording of the circumferential normal stress vs. position is given in Figure 9. Data taken from such a record, followed by differentiation, then gives the variation of circumferential shear stress with radius of curvature using the adjusted pressures given in Table I. This information is presented in Table VI.

TABLE VI

CIRCUMFERENTIAL SHEAR STRESS

Rib	Flywheel Diameter, in.				
	Flat Plate	192	120	84	67.3
1	100	99	108	115	113

It appears that in the case of circumferential shear stress the magnitude increases as the roadwheel size decreases in a manner similar to the case of the axial direction.

The general shear stress state associated with varying roadwheel curvature indicates that the plate condition has the lowest stress state.



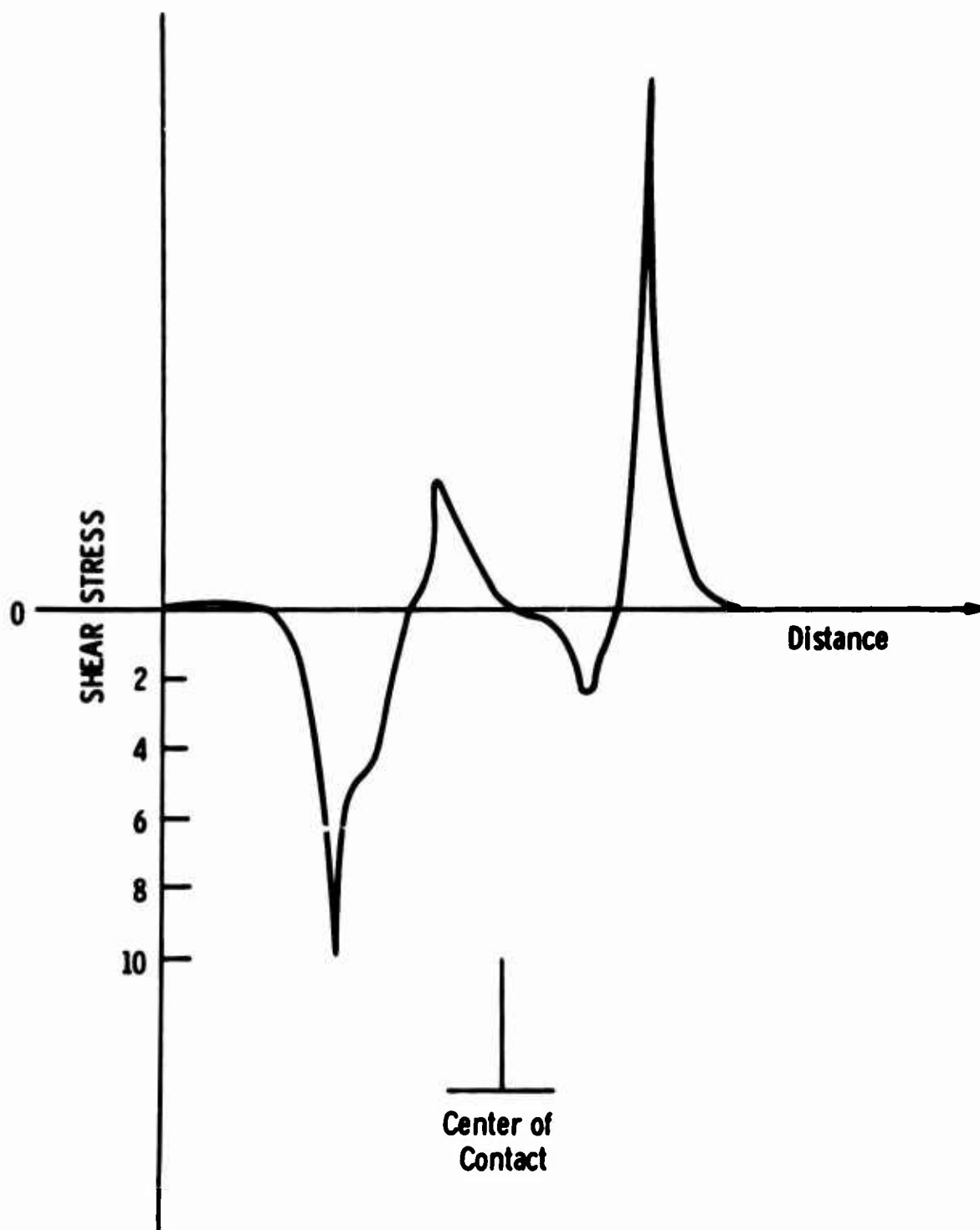


Figure 8. Circumferential Shear Stress at Tread Base as Tire Rolls Through Contact.

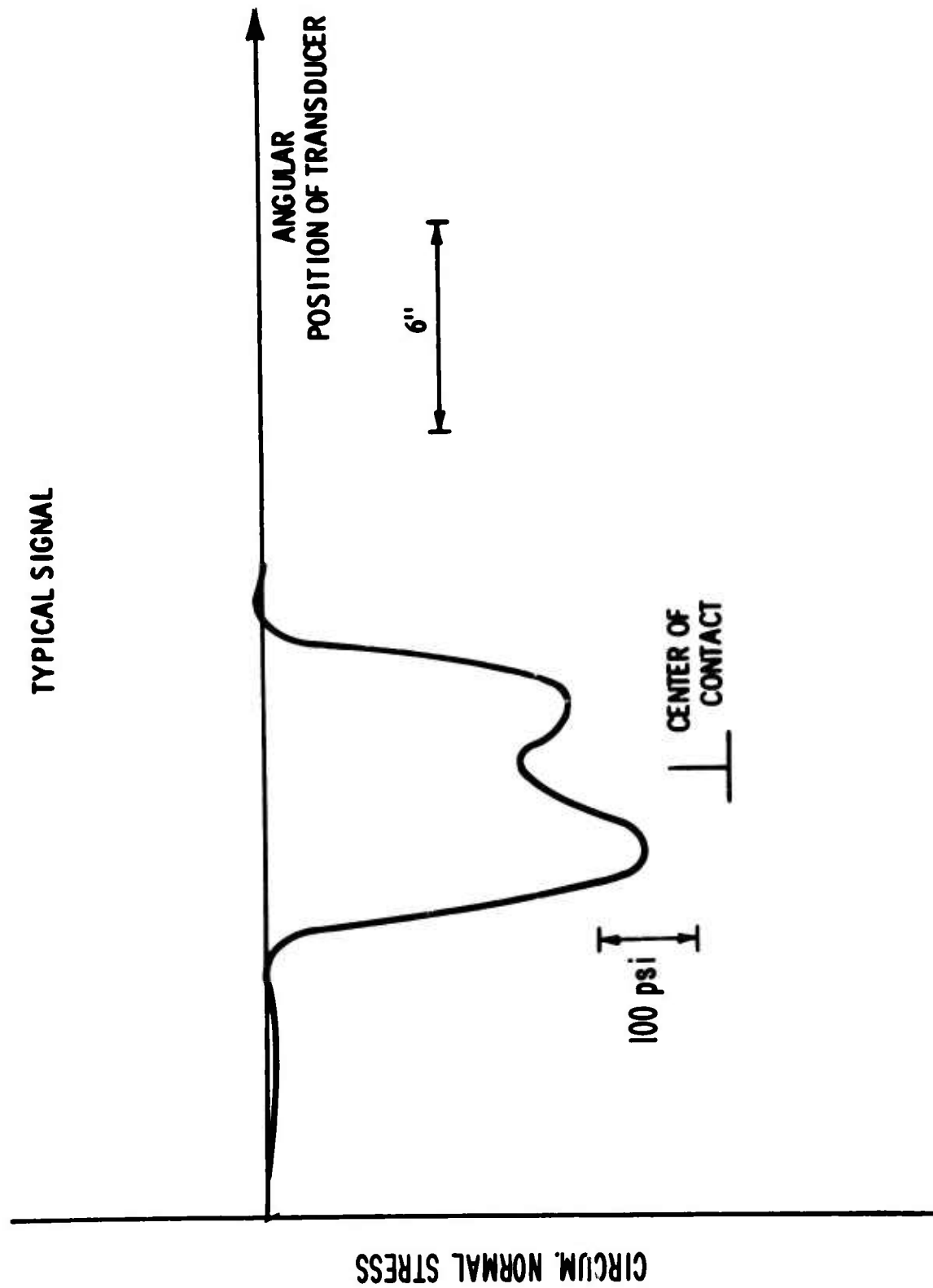


Figure 9. Circumferential Normal Stress vs. Position as Tire Rolls Through the Contact Patch.

## CORD LOAD MEASUREMENTS

It was initially planned to conduct series of cord load measurements using cord load transducers previously described in the literature [4]. One tire was especially constructed at the B. F. Goodrich Tire Company under subcontract from The University of Michigan using 33 cord load transducers designed to measure the cord tension throughout the body of the tire. Locations of these transducers were chosen in such a way that a complete section of a tread rib could be isolated all the way to the innerliner of the tire, in the sense that the cord loads on this section could be completely measured. The transducers were calibrated and the tire was built in March 1972. Several transducers were damaged during the tire curing process, and it was found that upon inflation of the tire a number of lead wires from other transducers also fractured. Less than half of the transducers remained workable after the lead wire failure, which was not anticipated prior to the tire building. In past experiences, the lead wires have functioned adequately under normal passenger car tire load and inflation conditions. Under the extremely high inflation pressures and large loads used by the 20 x 4.4 tire, lead wire fracture became a serious problem.

Since not enough cord load transducers were available to completely form a free body diagram of a section of the tread rib, other means had to be found to determine shear stress at the base of the tread and this was done using the shear stress transducers described in Appendix II. The remaining cord load transducers were recorded more out of general interest concerning the carcass fatigue life characteristics, rather than any direct attempt to measure the stress state at the base of the tread. The cord load transducers were calibrated and used in the normal way, and further details of their use may be found in Appendix III.

Cord load data was first obtained for the case of tire inflation only. This is presented in Figures 10, 11, 12, and 13, where cord load at various locations is plotted against inflation pressure. For most locations the cord load increases approximately linearly with pressure. For some locations the cord load drops as pressure increases and then rises almost linearly. This latter phenomenon has been previously observed on other tires, and can be explained by the fact that the tire changes shape as it initially inflates. As the pressure increases it reaches its equilibrium shape and from that point on the cord load is proportional to pressure.

A more detailed view of the transducer locations is given in Figure 14. A plot of the transducer output in strain units against cord load is given in Figure 15. This was obtained during calibration and is presented to illustrate the linearity of these measuring devices.

Data is next presented for cord loads in the tire carcass as the tire is operated against roadwheels of varying diameter under conditions shown in Table I, the modified MIL-T-5041F conditions. This is best seen by Figure 16, showing the decrease in contact patch length as radius of curvature decreases, and by Figures 17, 18, and 19. These latter three figures show that, as the radius of the roadwheel decreases, the following changes in cord load occur:

- (a) The maximum or peak cord load increases.
- (b) The minimum cord load remains nearly constant.
- (c) The alternating or fluctuating component of cord load increases.

This again points up the conclusion that the present schedules of adjustment of inflation pressure on different sizes of roadwheels are too severe for all road wheels, but particularly the smaller ones.

# CORD LOAD TRANSDUCERS

## Inflation Calibration

20 x 4.4

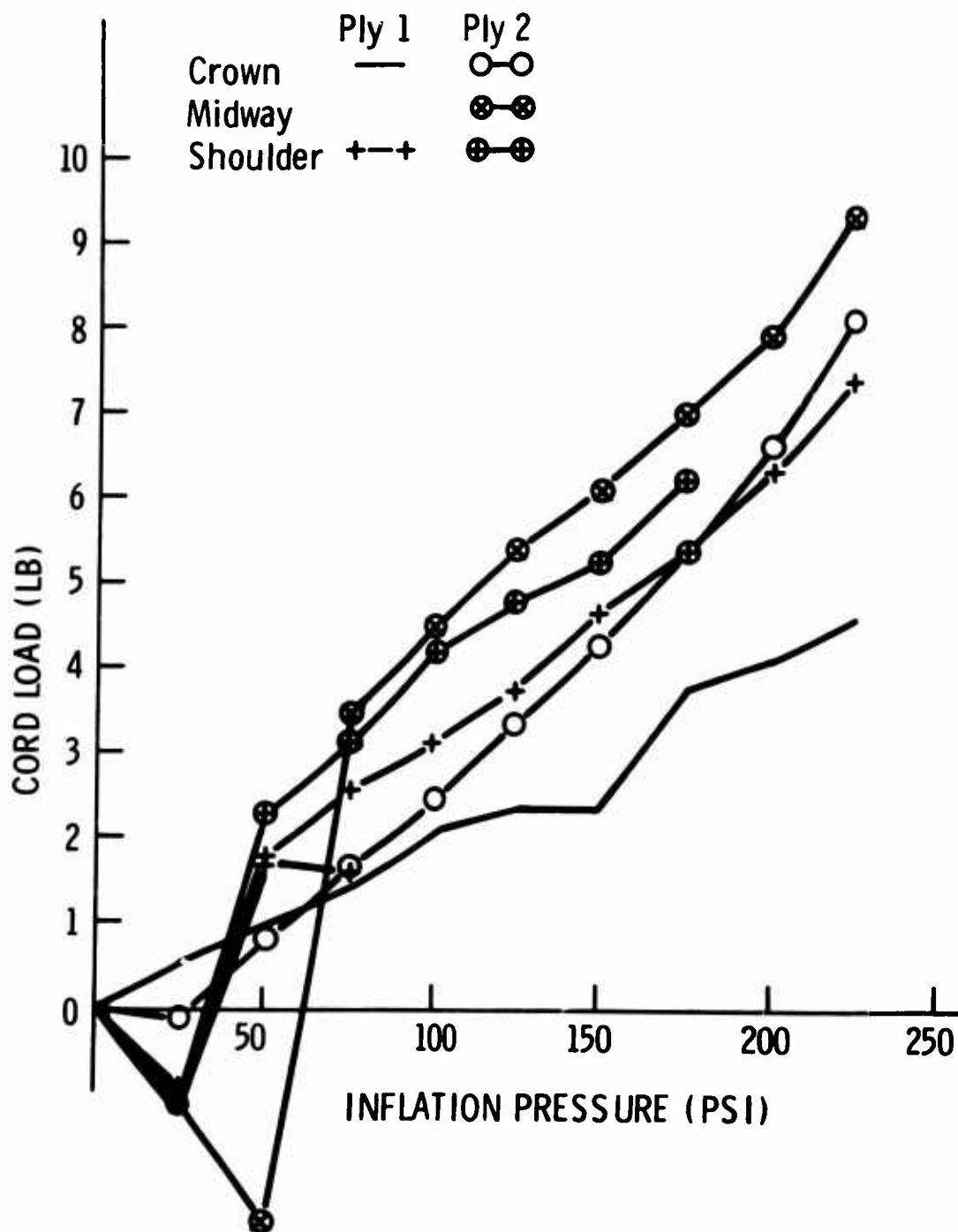


Figure 10. Cord Load vs. Inflation Pressure, Plies 1 and 2.

## CORD LOAD TRANSDUCERS

### Inflation Calibration

20 x 4.4

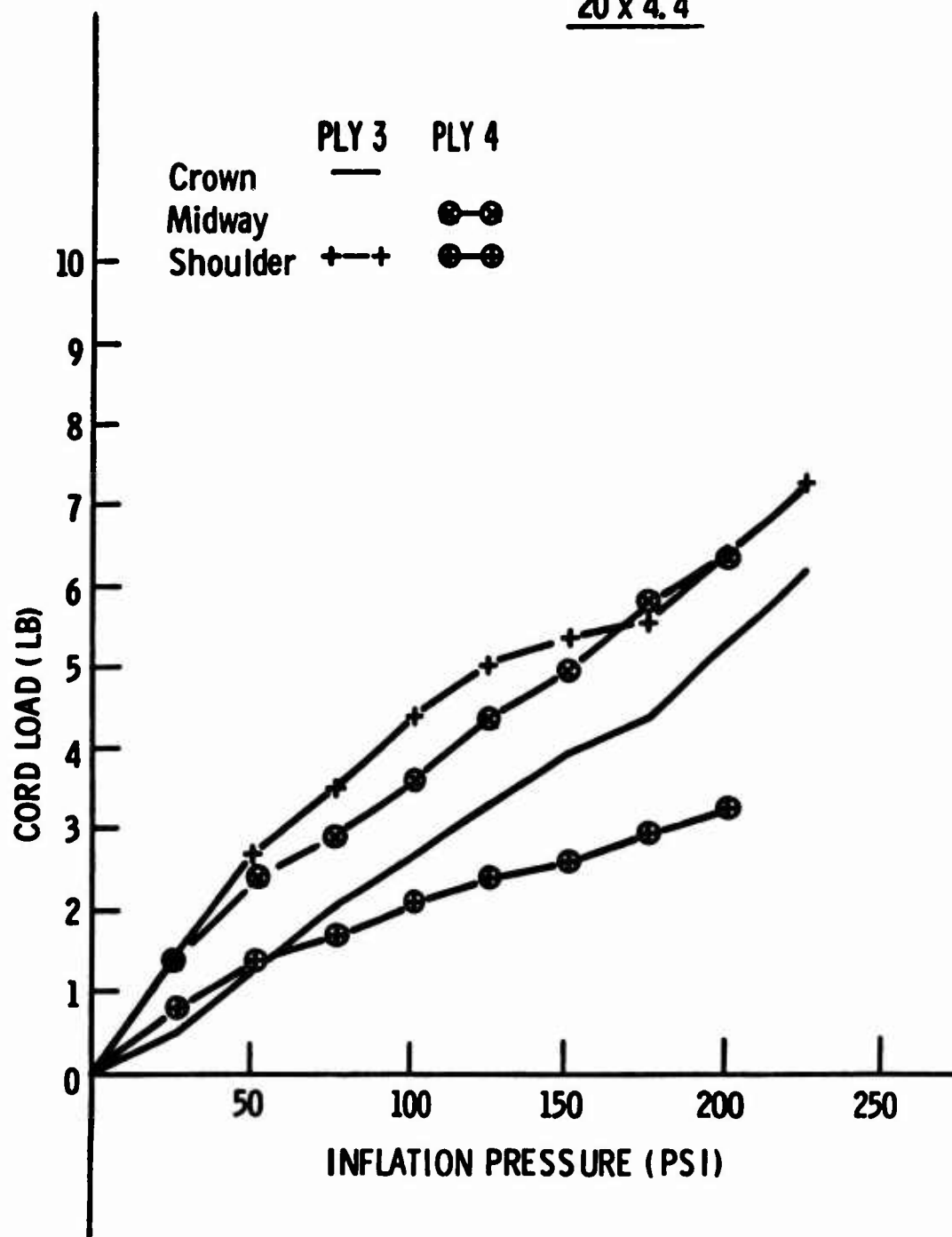


Figure 11. Cord Load vs. Inflation Pressure, Plies 3 and 4.

# CORD LOAD TRANSDUCERS

## Inflation Calibration

20 x 4.4

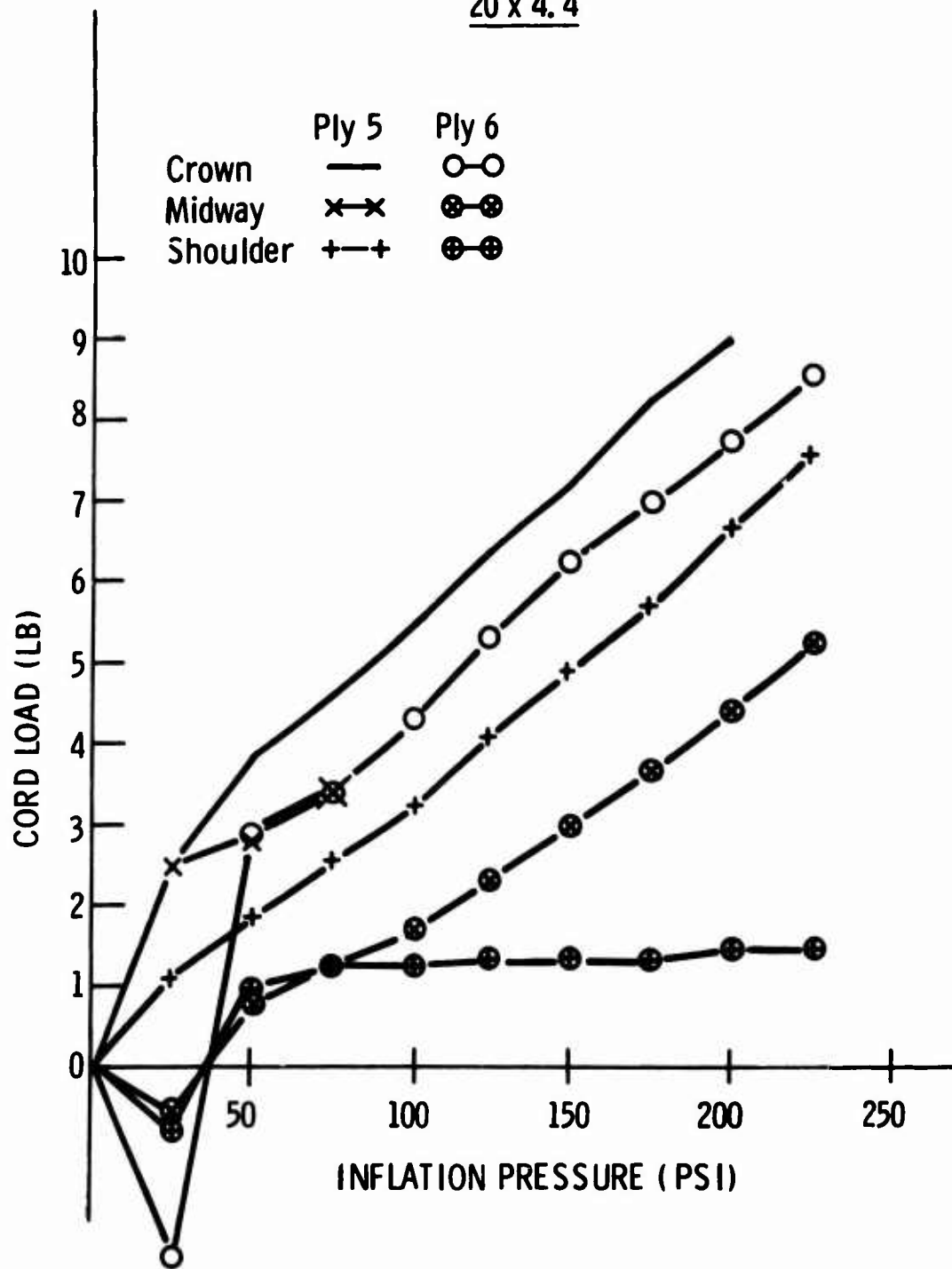


Figure 12. Cord Load vs. Inflation Pressure, Plies 5 and 6.

# CORD LOAD TRANSDUCERS

## Inflation Calibration

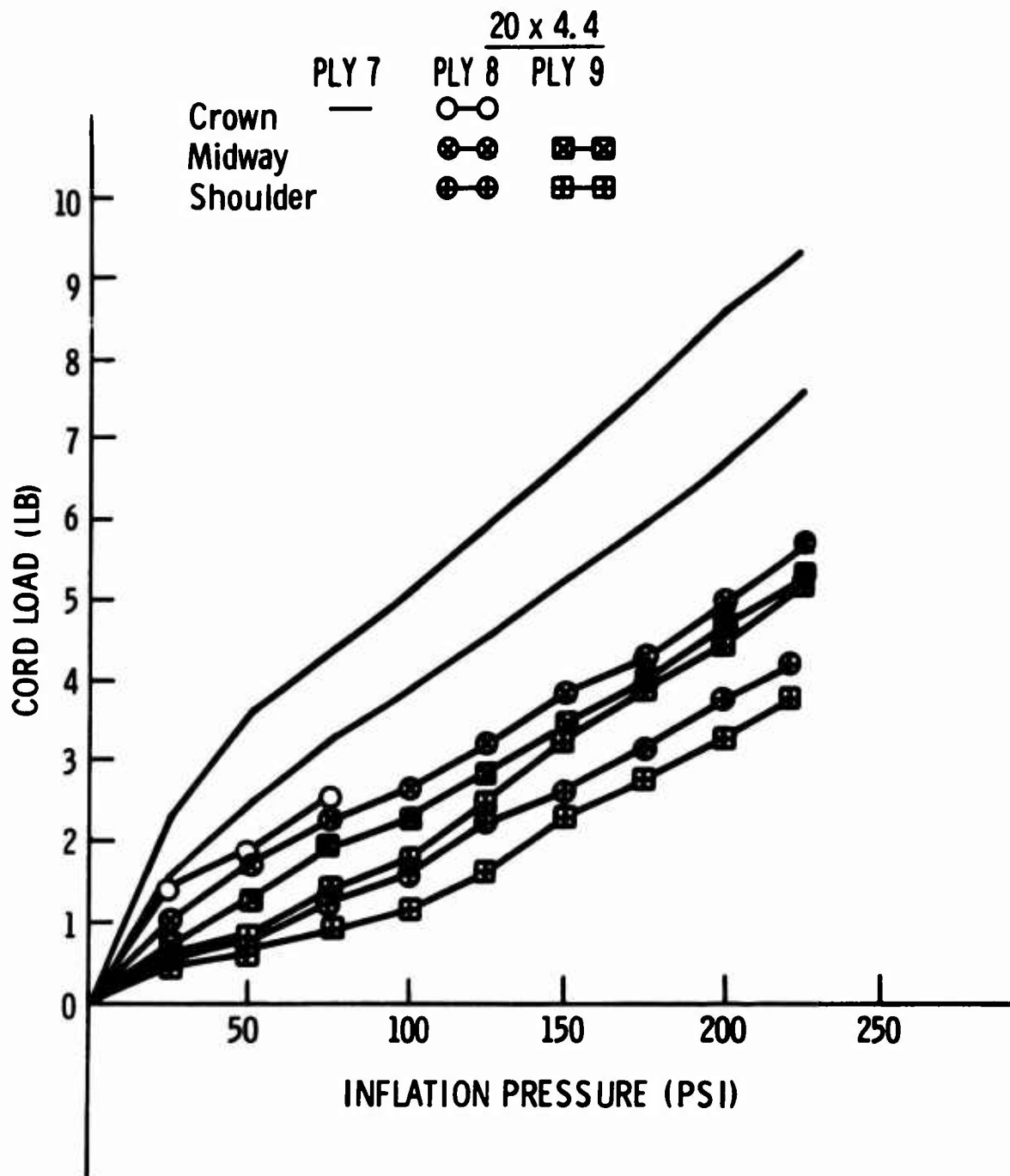


Figure 13. Cord Load vs. Inflation Pressure, Plies 7, 8, and 9.



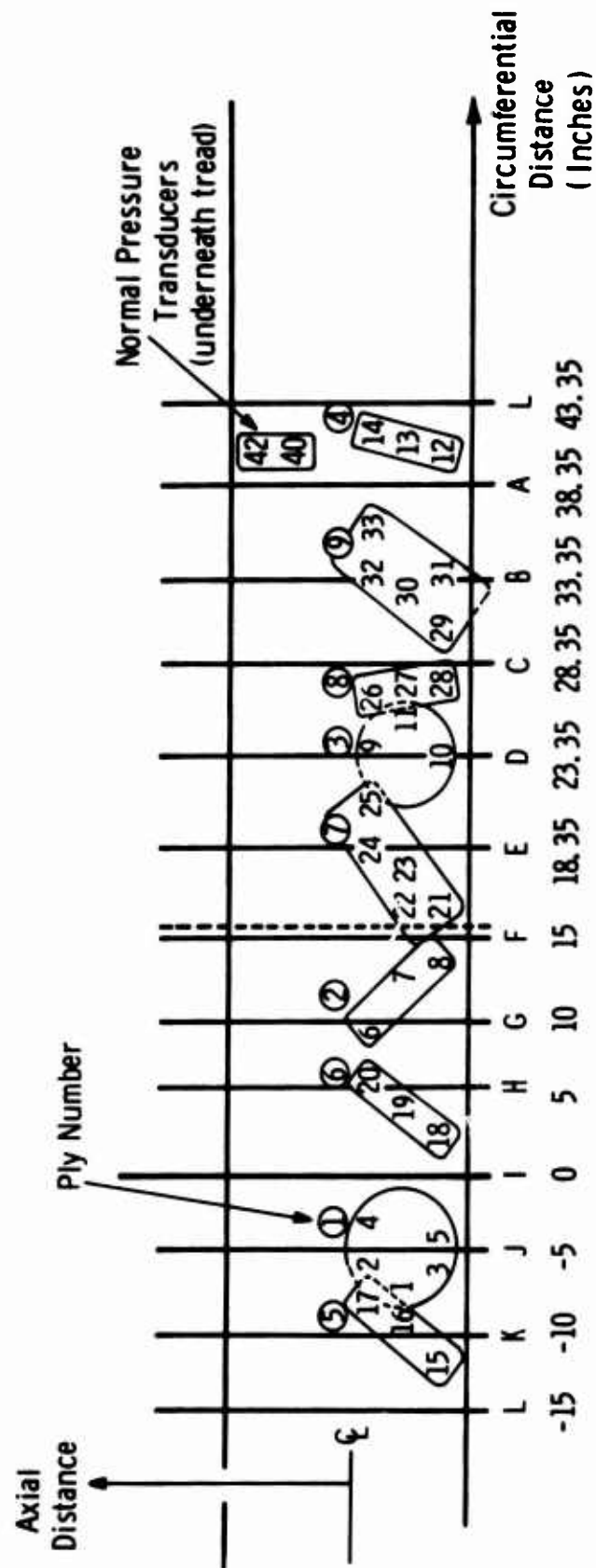


Figure 14. Cord Load Transducer Locations.

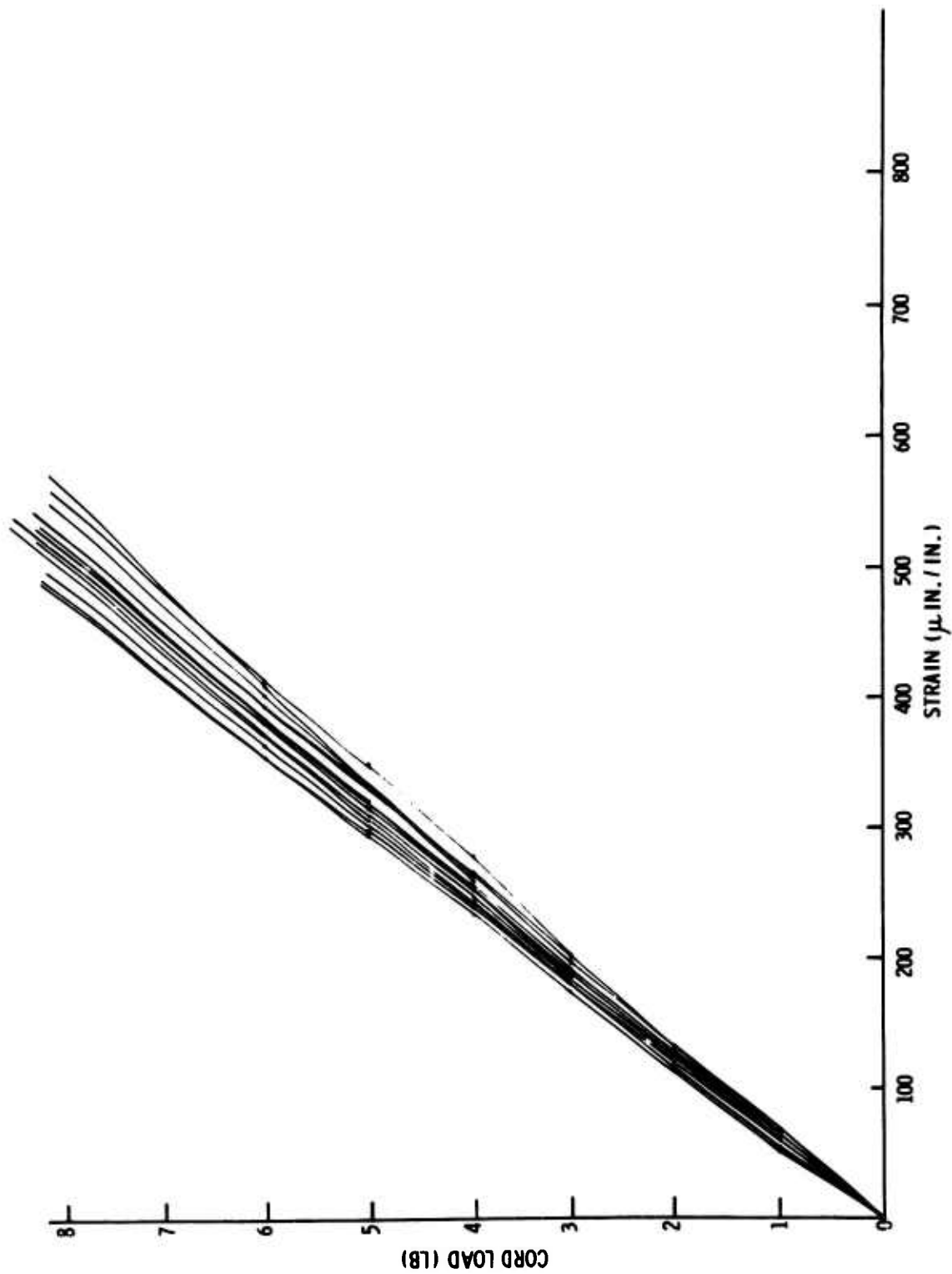


Figure 15. Calibration Of Cord Load Transducers—Output Signal vs. Cord Load.

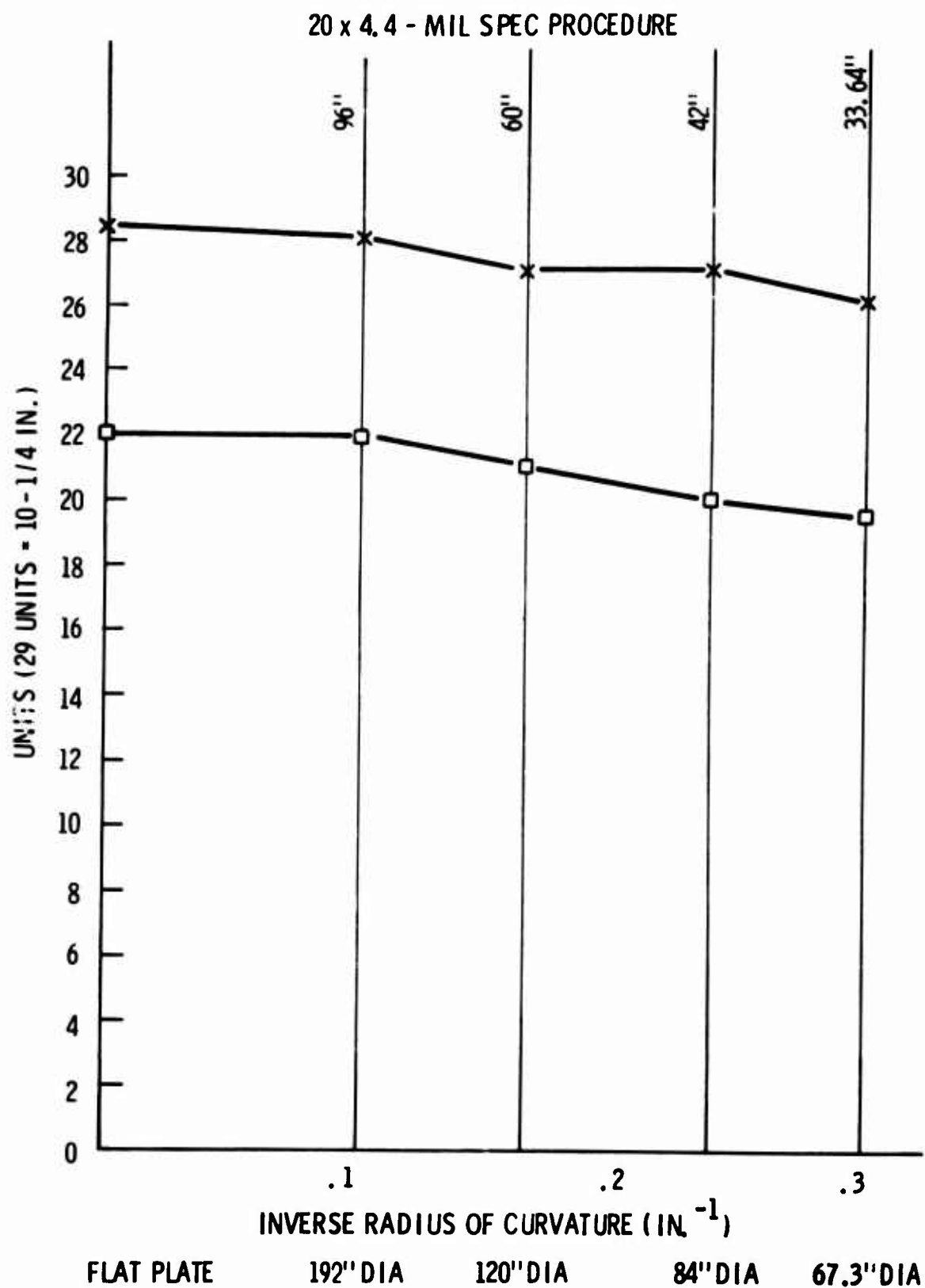


Figure 16. Contact Patch Length, as Measured by Signal Bandwidth from Cord Load Transducers, for Various Roadwheel Diameters.

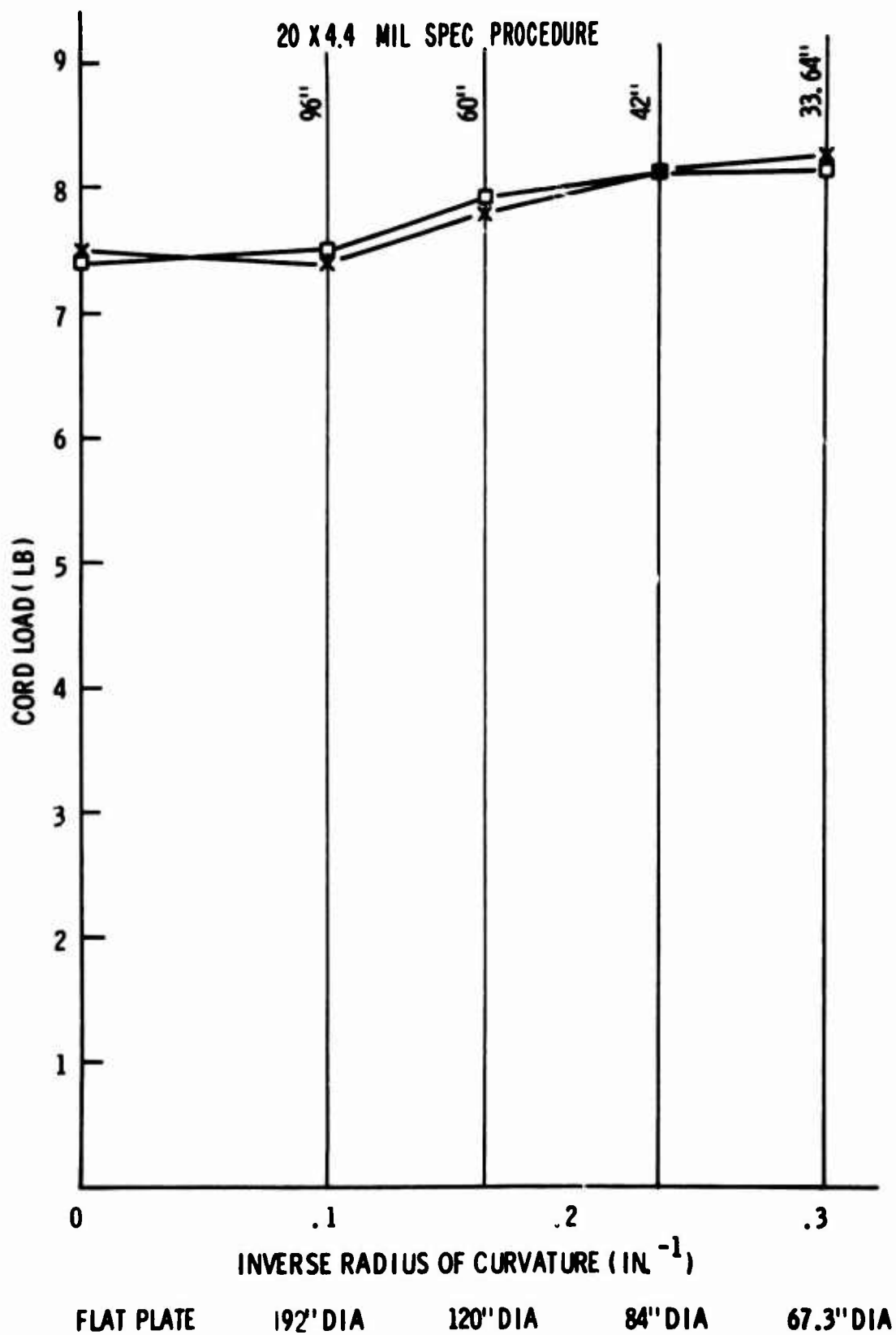


Figure 17. Peak Cord Load for Various Roadwheel Diameters.

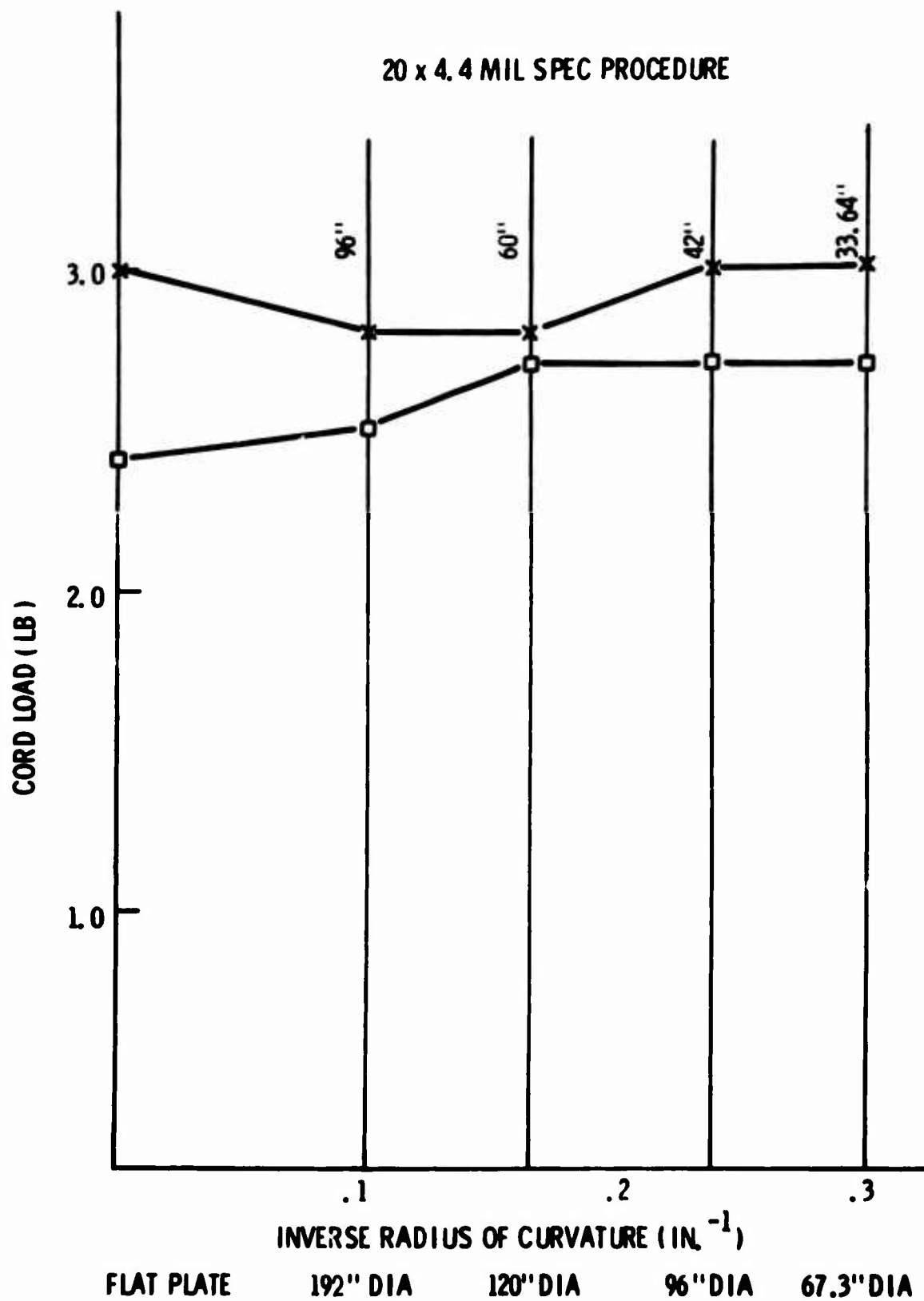


Figure 18. Minimum Cord Load for Various Roadwheel Diameters.

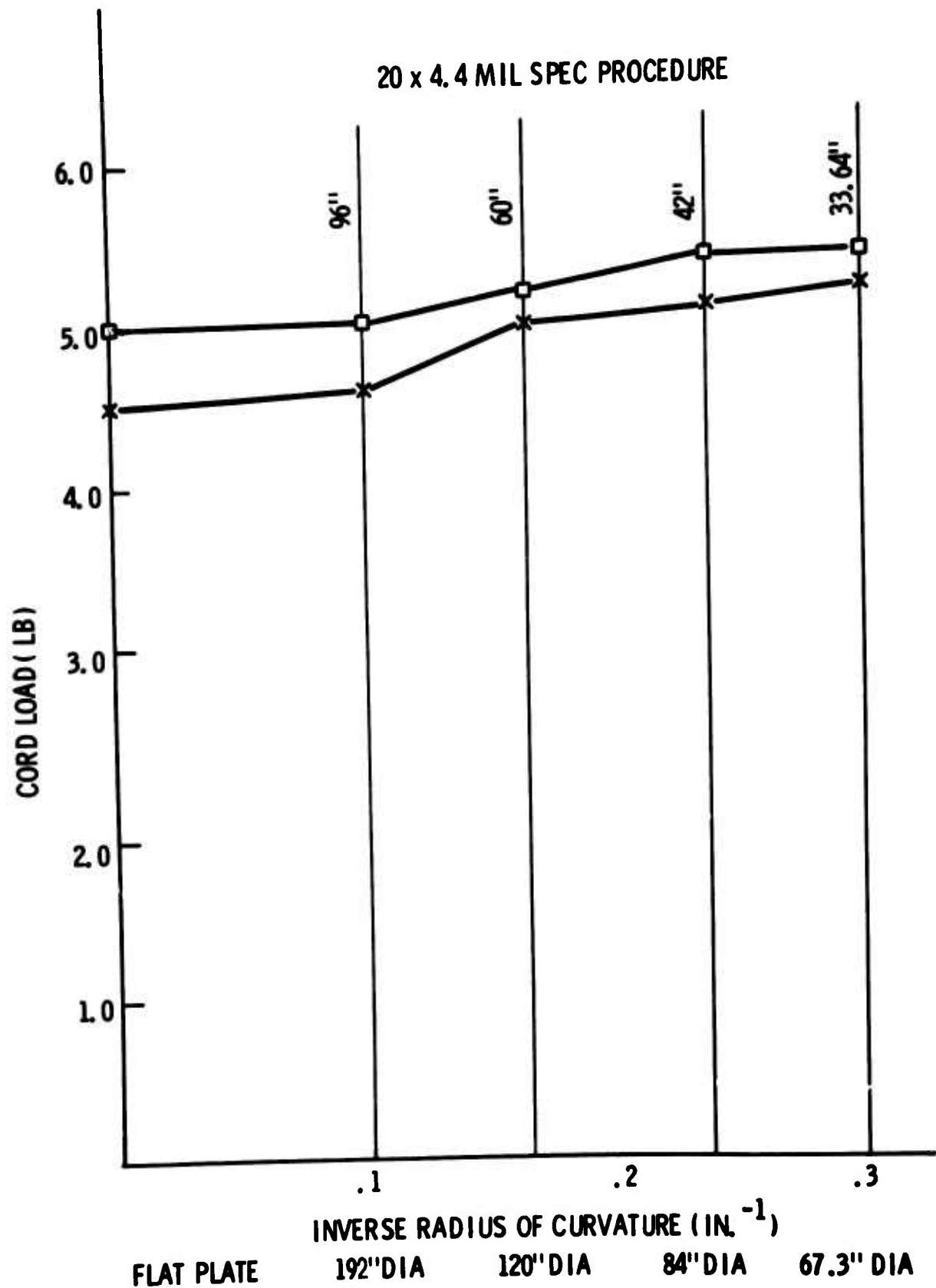


Figure 19. Alternating Cord Load for Various Roadwheel Diameters.

## TEMPERATURE MEASUREMENTS

One of the original objectives of the program was the measurement of tire temperatures at the base of the tread under conditions of take off and two-mile warm up on various diameters of roadwheels. Early efforts at the use of conventional thermocouple systems showed rather clearly that considerable development work would be needed in order to produce a lead wire system for thermocouples which would not fail prematurely in fatigue. Some temperature data was obtained using embedded thermocouples during two sets of tests using the 84-in. roadwheel at the Air Force Flight Dynamics Laboratory, Wright-Patterson Air Force Base. However, in both cases lead wires tended to fail quite early even in the case of the two-mile warm up test. Improvements were made in technique and in materials, but it became evident that in order to solve this problem of thermocouple lead wires a separate development effort would have to be instituted. For this reason it was jointly agreed between AFFDL and The University of Michigan that this section of the work should be deleted from the original contract. Thus only one set of results is given on temperature buildup at the base of the tread on this one roadwheel diameter, this is given in Figures 20 and 21.

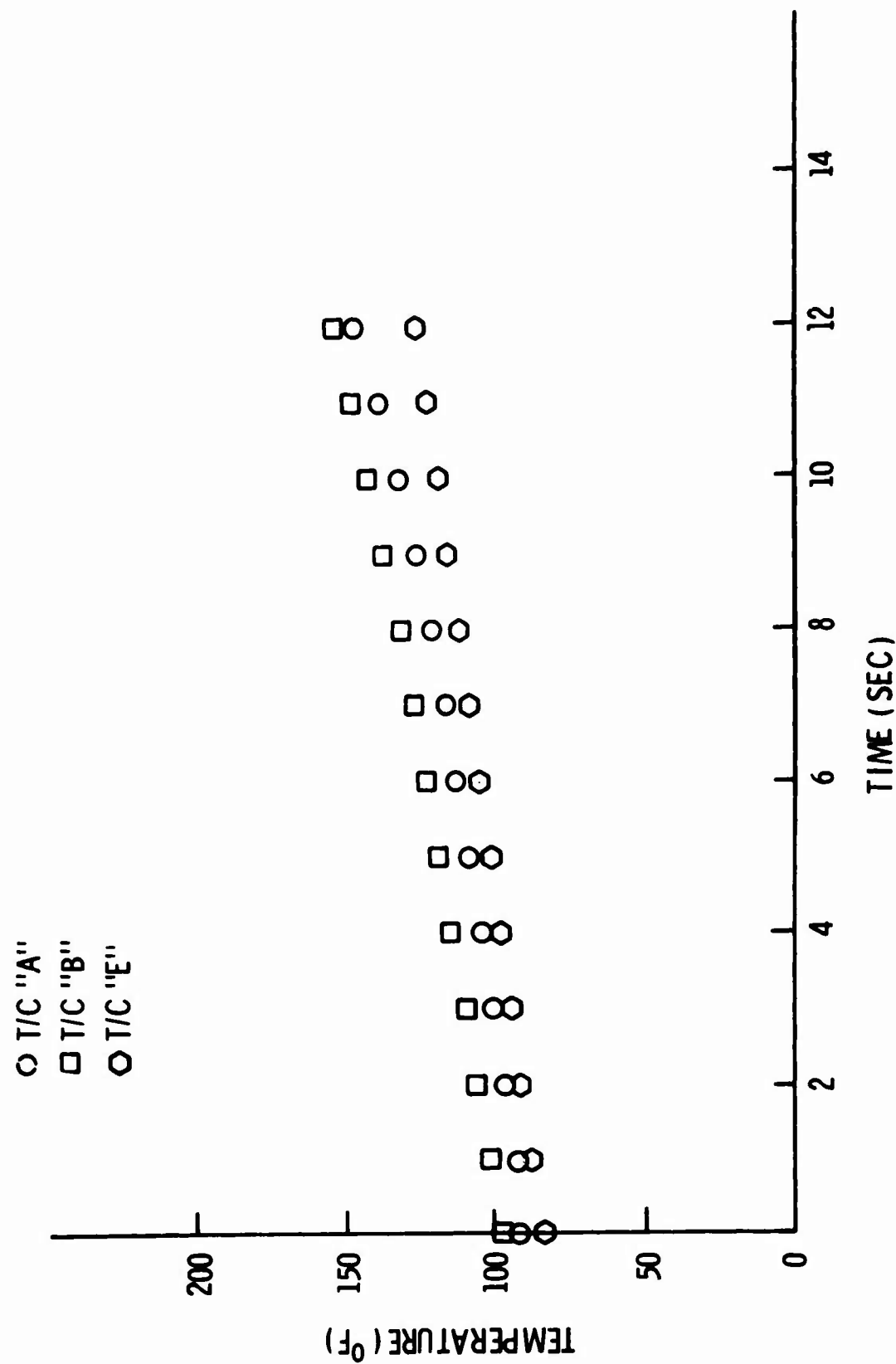


Figure 20. Tire Temperature Buildup During Taxi-Takeoff Cycle.



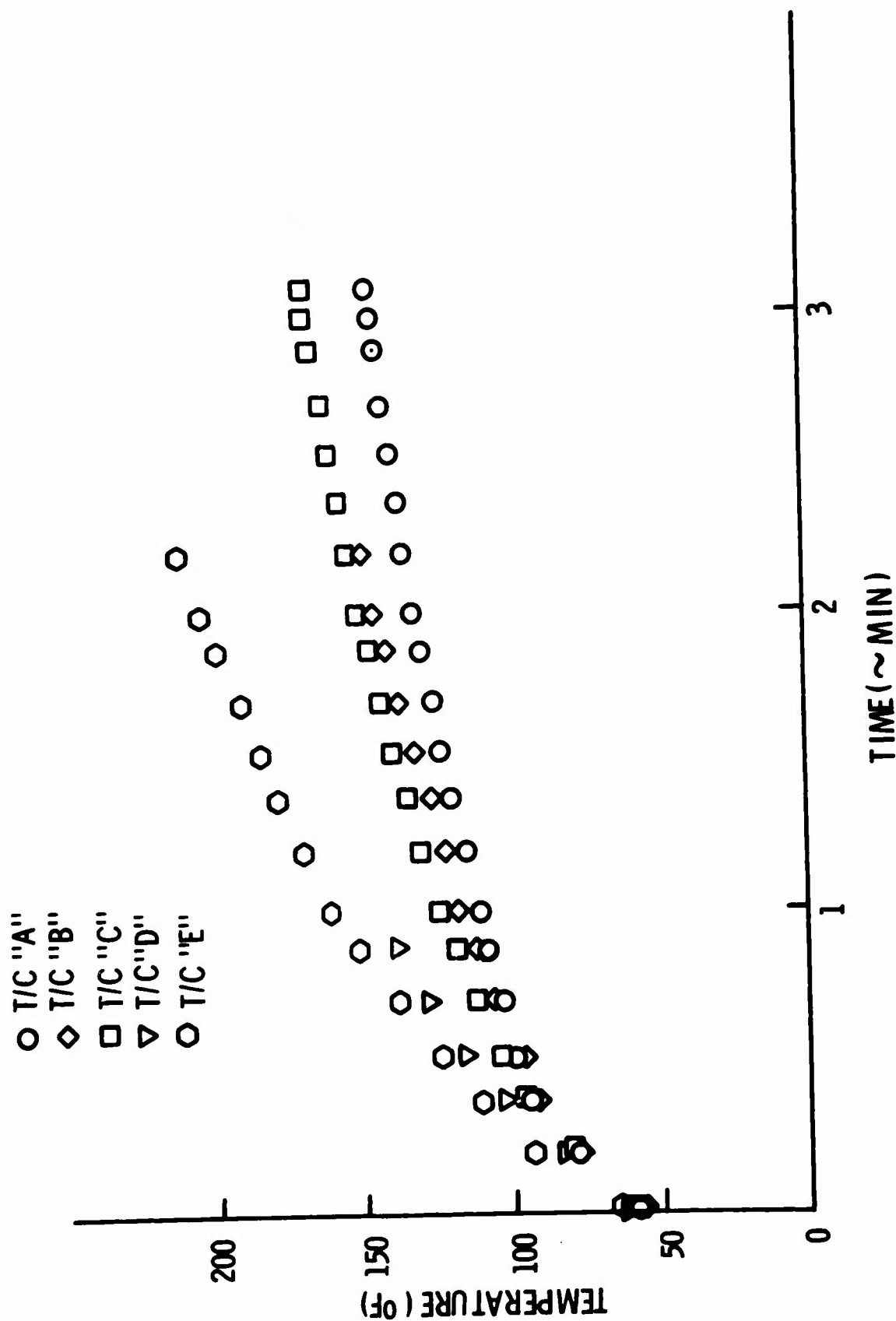


Figure 21. Tire Temperature Buildup During Two-Mile Break-In Run.

## SUMMARY OF STRESS STATE MEASUREMENTS

The normal and shear stress measurements made during the course of this program indicate very clearly that under the present schedule of inflation pressure and loading for the 20 x 4.4 tire, the stress state at the base of the tread increases approximately 20 percent during the transition from a flat plate inflation to an inflation suitable for a 67.30-in. roadwheel. Intermediate values of stress increase are approximately linear for intermediate values of flywheel curvature. Not all stress components increase in the same amount, but the two primary ones which seem to do so are the normal stress component perpendicular to the tread face and the shear stress component in the axial direction of the tire. The evidence concerning the shear stress component in the circumferential direction of the tire is not as strong, but it does seem to indicate some increase as roadwheel size decreases. No evidence is currently available on the relative temperatures under these various inflation schedules.

## CONCLUSIONS AND RECOMMENDATIONS

It is concluded that sufficient evidence has been found to cast some question on the validity of the present method for adjusting inflation pressure to account for varying diameters of test roadwheels. It is recommended that this type of program be repeated on a series of tire sizes, and that the results of these measurements be used to readjust the loading and inflation schedule for military aircraft tire qualification using variable diameter roadwheels.

#### REFERENCES

- [1] Kern, W. F., "Strain Measurements on Tires by Means of Strain Gauges." *Revue Generale du Caoutchouc*, Vol. 36, October 1959, pp. 1347-1365.
- [2] Janssen, M. L. and Walter, J. D., "Rubber Strain Measurements in Bias, Belted and Radial Ply Tires." Presented at Division of Rubber Chemistry, American Chemical Society, Miami Beach, Fla., 1971.
- [3] Walter, J. D., "A Tirecord Tension Transducer." *Textile Research Journal*, Vol. 39, Feb. 1969, p. 191.
- [4] Clark, S. K. and Dodge, R. N., "Correlation of Cord Loads in Tires on Roadwheel and Highway," SAE Paper 700093, 1970.
- [5] Dodge, R. N., Larson, R., and Clark, S. K., "Cord Load Measurements on Glass Belted Bias-Belt Tires with Polyester Carcass." Report prepared for Owens/Corning Fiberglas Corp., July 1971.
- [6] "Mechanics of Pneumatic Tires," N.B.S. Monograph No. 122. Government Printing Office, Washington, D.C., 1971.

## APPENDIX I

### NORMAL STRESS TRANSDUCERS

The normal stress transducers used in this work were of two different designs, each using the same mode of operation. The transducer itself is constructed of 0.005-in. thick beryllium copper sheet which is formed into the shape of a recessed diaphragm of approximately 0.100 in. in diameter, with an overall outside diameter of 0.125 in. A single foil resistance strain gage is mounted on the inside surface of one of the two formed pieces which are tightly bonded together to form a hollow case similar in construction to a watch case. The completed transducers have an overall thickness of 0.030 in. The transducer is sensitive to compression or tension perpendicular to its face, and by using a known calibration curve connecting the output signal to the imposed stress, these transducers may be used to determine the internal normal stresses in deformable materials. The assembled transducer is shown in Figures 22 and 23.

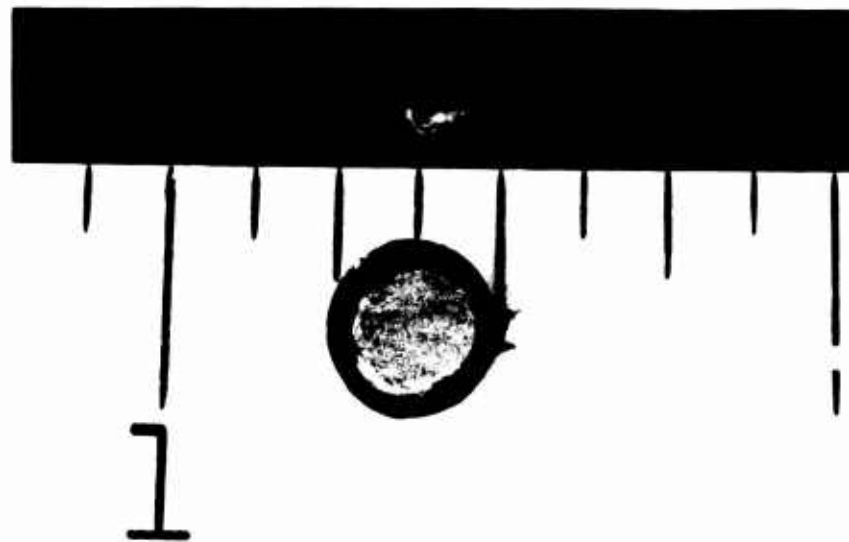


Figure 22. Sensing Face of Normal Stress Transducer.



Figure 23. Edge View of Normal Stress Transducer.

In order to investigate the relation between transducer output and normal stress, typical transducers were installed in several simple elastic bodies whose stress state under known loadings could be calculated. In one case, the transducers were embedded in a molded rectangular beam of silicone rubber. In this configuration, the response to bending, torsion, tension, and shear could be examined. For example, when the beam was placed in a state of pure bending the transducer output was essentially zero as would be expected. A similar result was found when the beam was placed in a state of torsion, since the transducer was oriented in such a way that the normal stress on its face under this simple loading condition was zero. On the other hand, when the beam was placed vertically as in a tension bar and placed in tension or compression, then the transducer signal was quite large and linearly proportional to the applied load. This was to be expected since the plane of the transducer was perpendicular to the axis of the beam.

In one other method of calibration, which was used for purposes of this report, the transducer was placed in a special tubular fixture which allowed it to be compressed between two cured rubber plugs restrained by a lubricated cylindrical guide. This guide was needed in order to minimize the lateral expansion effects of the rubber plug, which tended to induce severe frictional forces on the face of the transducer and to alter the normal stress distribution between the two mating rubber plugs. The resulting calibration was done by plotting the average stress applied to the face of the upper rubber plug against the signal output of the transducer. The two quantities were reproducible and linear to within 1 percent up to 300 psi. This calibration system is illustrated in Figure 24. The slope of the resulting plot gave the

calibration factor connecting the mean stress of an embedded transducer to its signal output. For the transducers used in this work, this value was approximately  $2 \mu\text{in./in./psi}$ . The tensile calibration was assumed to have the same value as that of the compression characteristics.



Figure 24. Calibration Fixture for Normal Stress Transducer, Disassembled.

Several of the transducers were calibrated hydrostatically. The resulting calibration factor was approximately 0.75 that of the calibration factor obtained by compressing the transducer between two rubber plugs as just described. This calibration factor was not used because it was felt that it was not compatible with the intended use of the transducer, since when molded in rubber the general stress state is not that of the hydrostatic compression.

The installation of the transducers on the buffed tire carcass presented potential problems of lead wire breakage. This was solved by lubricating the lead wires with silicone grease after the transducers were bonded to the surface of the buffed tire and before tire recapping took place. In general this was sufficient to prevent leadwire fracture.

## APPENDIX II

### SHEAR STRESS TRANSDUCERS

One type of shear stress measurement made for this study involved the use of a shear stress transducer specifically designed and developed for this work. This stress transducer used the concept of measuring the angular deformation of a small beryllium copper beam bent at right angles with a radius of curvature at the intersection of the two arms. Foil strain gages were placed at this radius of curvature connecting the two arms. This geometry is illustrated in Figure 25. The strain gages shown there were connected in series so as to measure only the bending effects associated with the deformation of the two arms, thus giving a signal proportional to the change in angular orientation of the two arms. The completed transducers were approximately 0.20 in. high and 0.075 in. wide. Again the gage material was beryllium copper. A photograph of the completed transducer is shown in Figure 26.

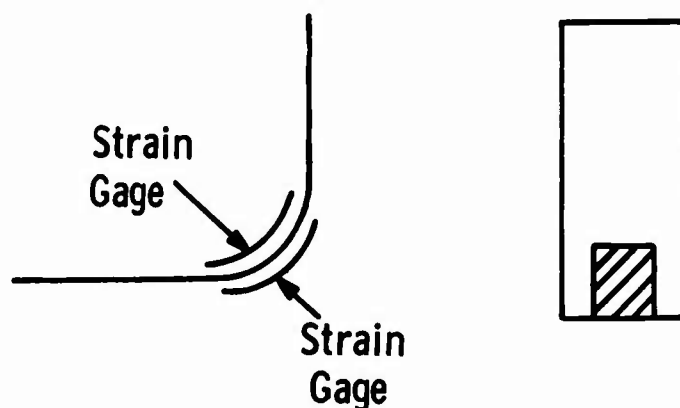


Figure 25. Shear Stress Transducer Geometry.

The completed transducers were molded in castable rubber plugs so as to insure proper orientation upon installation, as well as to protect the transducer from possible damage during installation. Again, these transducers were installed in several simple elastic shapes in order to investigate the nature of the signal from them as a function of loading. Probably the most effective of these shapes was an annulus of cured rubber loaded in pure torsion. This was designed to examine the linearity of the transducer with respect to shear stress. This fixture is illustrated in Figure 27. The results of the tests in pure torsion were encouraging, since the signal there is linear, repeatable and proportional to the shear deformation. However, no direct attempt was made to assign a specific calibration factor to this type of experiment since it was very difficult to recover each individual transducer after bonding it to the rubber annulus.



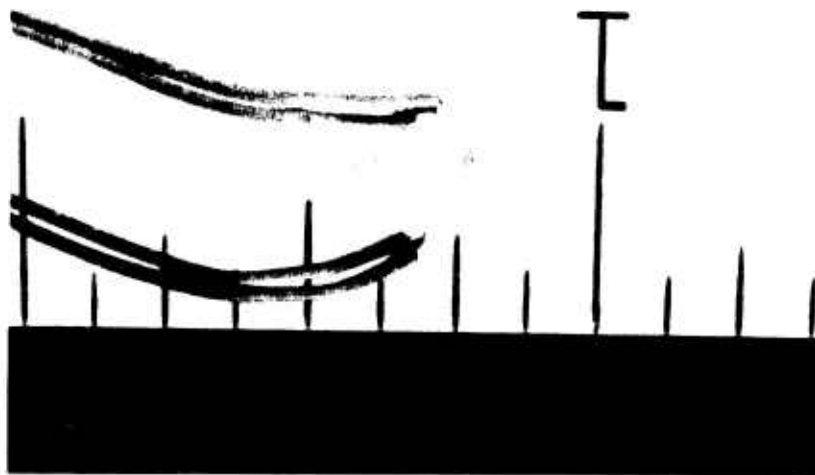


Figure 26. Photograph of Shear Stress Transducer.



Figure 27. Shear Stress Calibration Fixture.

In order to determine the transducer response to other types of loading, one of these transducers was also molded into a silicone rubber beam as shown in Figure 28. This beam was subjected to torsion tests perpendicular to the axis of the transducer, to tension and to compression. All the resulting signals were very small, indicating that the transducer was insensitive to normal strains or dilatation.

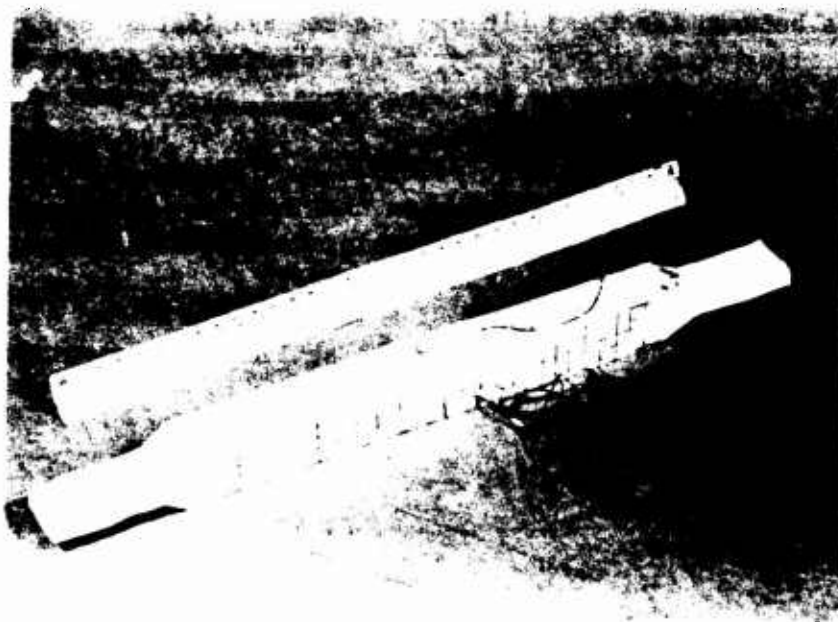


Figure 28. Rubber Beam Used to Calibrate Shear Stress Transducers.

Following these checks on the transducer effectiveness, several transducers were installed in the recapped 20 x 4.4 tire. This was done by first molding the transducer into a castable rubber plug, and then bonding these plugs to the buffed surface of the tire just prior to recapping. The transducer was then encapsulated with skim stock and the lead wires lubricated with silicone grease as described in encapsulating the normal stress transducers. The tread of the tire was then applied and the tire was cured by the usual processes.

The resulting signals from the shear stress transducers are only of comparative value and cannot be interpreted in terms of absolute shear stresses. Nevertheless, they are of value since they determine the relative shear strains and hence relative shear stresses while the 20 x 4.4 tire is operating on simulated roadwheels of different diameter.

### APPENDIX III

#### CORD LOAD TRANSDUCERS

One of the original concepts used in this work was that measurement of cord load in a small controlled volume could lead to a knowledge of the average shear stress between the tread rib and the carcass in that control volume. This concept is illustrated in Figure 29, where a number of arrows indicate cord loads which may be measured in the tire carcass, over a section of length  $\Delta x$  in the circumferential direction equal to the width of the tread rib in the axial direction. A complete knowledge of these cord forces should allow one to determine the average shear stress  $\tau_{zx}$  on the interface between the tread and the tire carcass, since the shear stress  $\tau_{zx}$  is the only unknown in the circumferential force equilibrium as shown in Figure 7. The implementation of such a calculation requires measurement of a fairly large number of cord forces, since the 20 x 4.4 tire utilizes eight active load carrying textile plies.

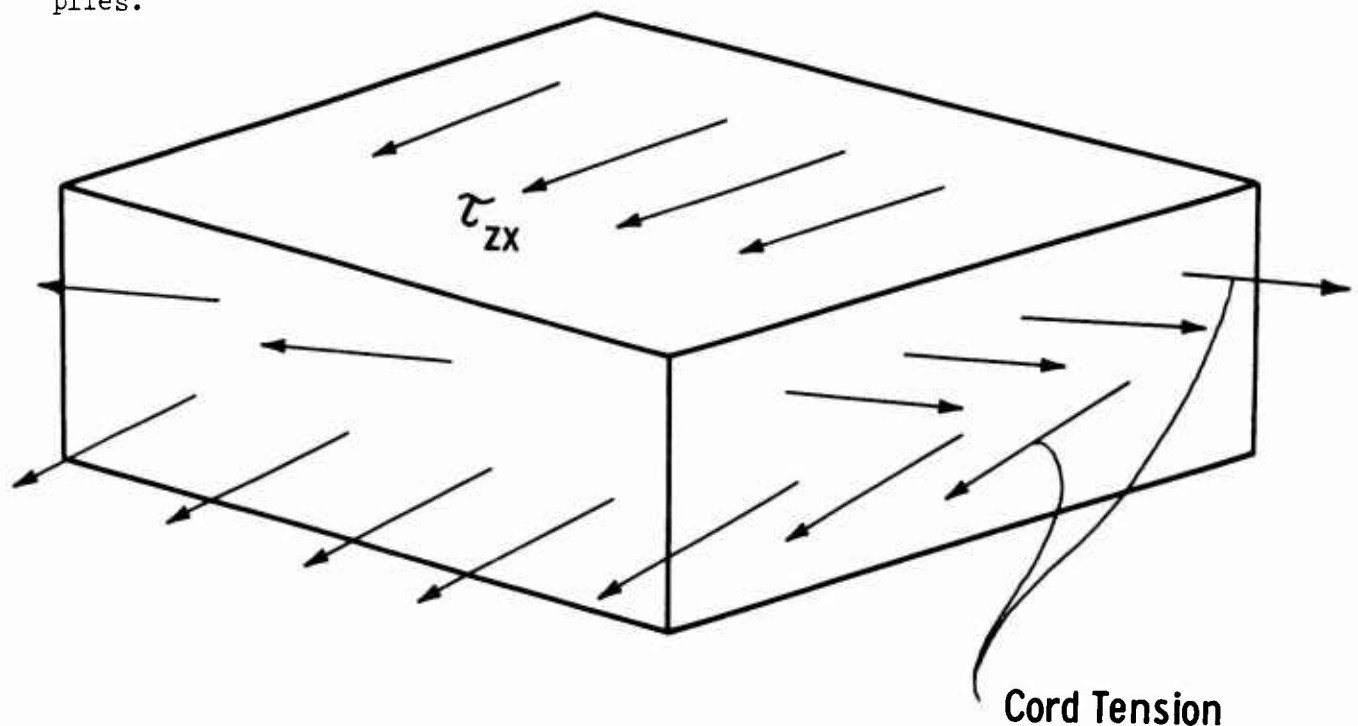


Figure 29. Free Body Diagram of Section of Tire Carcass.

Isolation of a section in the tire in the region of rib 1, as defined in Figure 29, led to the conclusion that at least 33 separate cord load transducers would have to be installed in the tire in order to obtain the information necessary to determine equilibrium as shown.

The cord load transducers chosen for this work were the conventional tubular type, and were manufactured of thin walled beryllium copper tubing using conventional foil resistance strain gages. Their design is illustrated in Figure 30. The transducers were attached to the individual cords, in this case 840/2 nylon, by means of a special high-temperature epoxy. Each transducer was individually calibrated and then each cord was carefully laid back into the rubberized fabric used for the construction of the tire carcass plies.

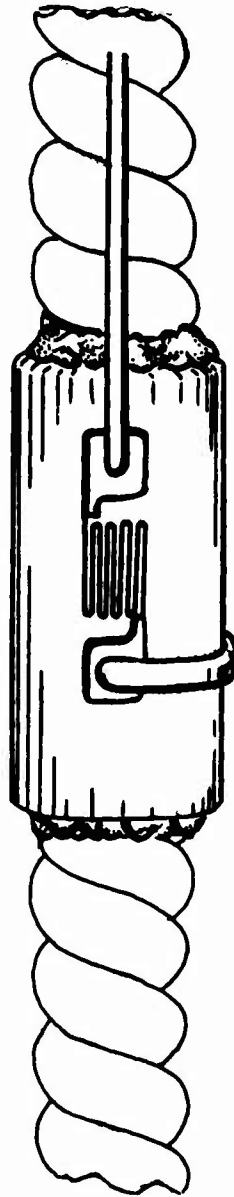


Figure 30. Tubular Cord Load Transducer.

#### APPENDIX IV

#### SIMULATED FLYWHEEL

For the purposes of the work described here, the 20 x 4.4 tire was to be tested on roadwheels of varying diameter at slow speed. Due to the fact that most of the tests required a laboratory setting to assure careful control of tire load, tire deflection and instrumentation characteristics, a method was devised for producing an artificial curved surface that simulated a steel roadwheel. This process involved loading the tire against a fixed contoured shoe of known and controlled radius of curvature as shown in Figure 31.

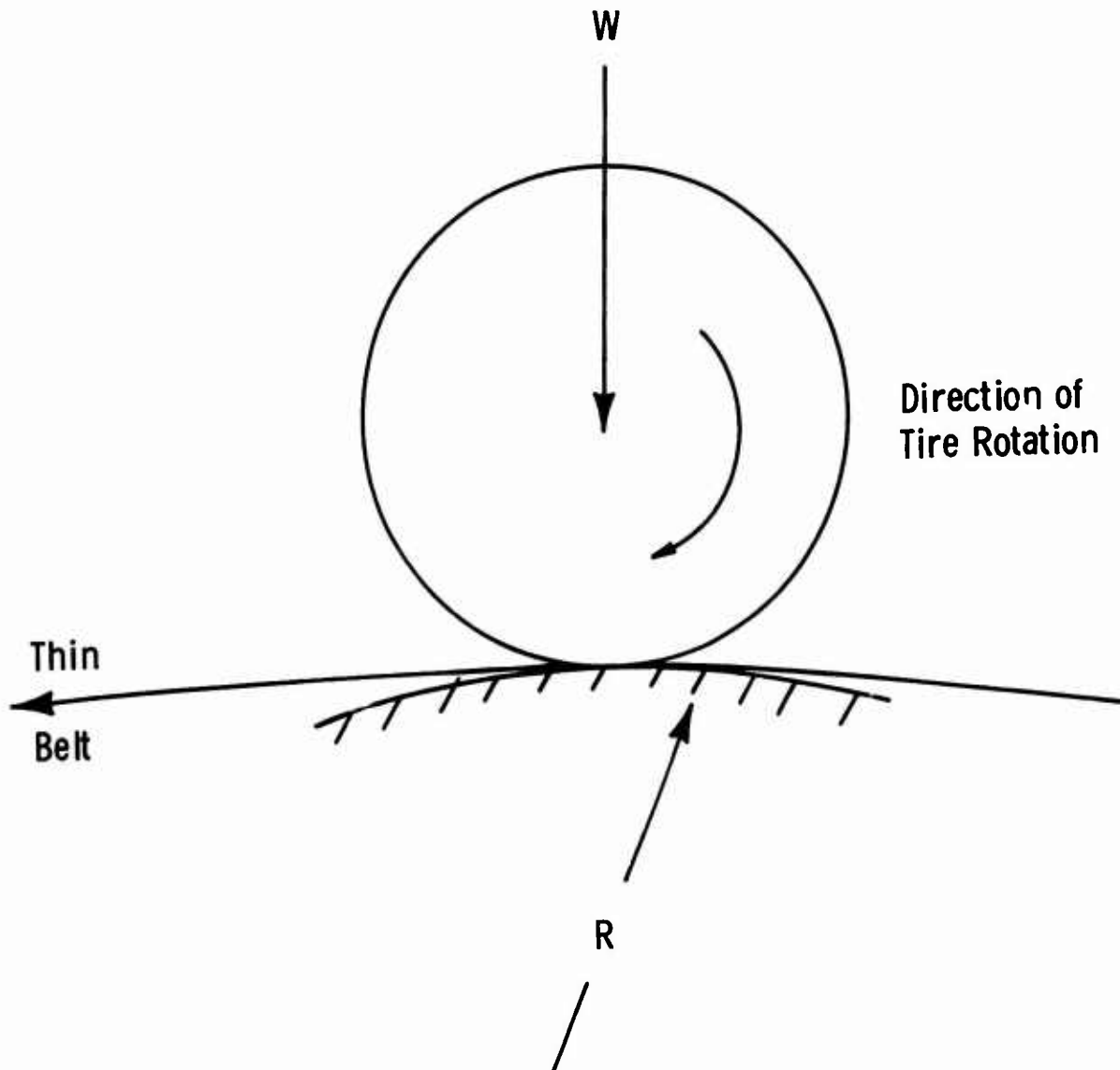


Figure 31. Schematic Drawing of Device to Simulate a Roadwheel.

Between the loaded tire and the fixed contoured shoe were three layers of material somewhat wider than the tire itself. The first layer beneath the tire was a thin sheet of aluminum of approximately 0.020 in. thickness which served the purpose of providing a friction surface having a friction coefficient essentially the same as that of a steel faced roadwheel. Directly under the aluminum sheet was a Teflon sheet of approximately 0.040 in. thick and approximately 8 ft long. Beneath this layer of Teflon was another sheet of Teflon fixed to the contoured shoe.

The test was conducted by pulling the long Teflon sheet between the contoured shoe and the tire. The Teflon, having very low friction coefficient, causes the aluminum sheet to be drawn between the shoe and the tire also. The tire, fixed vertically and longitudinally, rotates, thus allowing the instrumentation in it to be monitored as this instrumentation rolls through the region of contact.

The Teflon sheet was pulled by means of a gear reducer and chain assembly with one end of the chain fixed to the long Teflon sheet.

The instrumentation embedded in the tire consequently reflects the internal stress state of the tire when rolling over an aluminum roadwheel with a diameter the same as that of the contoured shoe. A photograph of this apparatus is shown in Figure 32.

By using this simulated dynamometer wheel the experiment can be carried out in the laboratory where careful control of the instrumentation and physical characteristics can be accomplished without requiring the costly use of test dynamometers for lengthy periods of time. The use of the laboratory also permits the addition of extra equipment necessary to control all of the variables of the experiment, thus avoiding the requirement of modifying expensive test dynamometers.



Figure 32. Photograph of Test Tire Loaded Against a Simulated Roadwheel.

~~Security Classification~~  
Unclassified

14. KEY WORDS	LINK A		LINK B		LINK C	
	ROLE	WT	ROLE	WT	ROLE	WT
aircraft tires						
strain transducers						
roadwheel testing						



Unclassified  
Security Classification

DOCUMENT CONTROL DATA - R & D		
<i>(Security classification of title, body of abstract and indexing annotation must be entered when the overall report is classified)</i>		
1. ORIGINATING ACTIVITY (Corporate author) The Regents of The University of Michigan Ann Arbor, Michigan 48104		2a. REPORT SECURITY CLASSIFICATION Unclassified
		2b. GROUP Not applicable
3. REPORT TITLE  Measurement of Stress States in 20 x 4.4 Aircraft Tire		
4. DESCRIPTIVE NOTES (Type of report and inclusive dates) Technical Report		
5. AUTHOR(S) (First name, middle initial, last name)  Samuel K. Clark, Richard N. Dodge, Donald Lee, and Richard Larson		
6. REPORT DATE February 1973	7a. TOTAL NO. OF PAGES 56	7b. NO. OF REFS 6
8a. CONTRACT OR GRANT NO. F33615-72-C-1004	8b. ORIGINATOR'S REPORT NUMBER(S)  010584-1-T	
8c. PROJECT NO.	8d. OTHER REPORT NO(S) (Any other numbers that may be assigned this report) AFFDL-TR-73-24	
9. DISTRIBUTION STATEMENT  Approved for public release; distribution unlimited.		
11. SUPPLEMENTARY NOTES  Not applicable	12. SPONSORING MILITARY ACTIVITY Air Force Flight Dynamics Laboratory Air Force Systems Command Wright-Patterson Air Force Base, Ohio	
13. ABSTRACT  Measurements were made on the stress state of the tread carcass interface on a 20 x 4.4 Type VII 12 PR aircraft tire operating on curved surfaces simulating a number of different roadwheel diameters. The general results of these measurements show that the stress levels in the tire increase as the roadwheel diameters decrease, using the adjusted pressure schedules given in Figure 5 of MIL-T-5041F, and that in all cases the stress levels are higher on curved roadwheels than on a flat surface such as a runway.		

DD FORM 1473  
1 NOV 65

14

Unclassified  
Security Classification